

UNCLASSIFIED

AD 410851

DEFENSE DOCUMENTATION CENTER

FOR

SCIENTIFIC AND TECHNICAL INFORMATION

CAMERON STATION, ALEXANDRIA, VIRGINIA



UNCLASSIFIED

NOTICE: When government or other drawings, specifications or other data are used for any purpose other than in connection with a definitely related government procurement operation, the U. S. Government thereby incurs no responsibility, nor any obligation whatsoever; and the fact that the Government may have formulated, furnished, or in any way supplied the said drawings, specifications, or other data is not to be regarded by implication or otherwise as in any manner licensing the holder or any other person or corporation, or conveying any rights or permission to manufacture, use or sell any patented invention that may in any way be related thereto.

410851

CATALOGED BY DDC

AS AD No. \_\_\_\_\_

410851

AFSWC-TDR-63-49

SWC  
TDR  
63-49

RESEARCH STUDY ON THE SURFACE INITIATION OF EXPLOSIVES

Final Report

June 1963

TECHNICAL DOCUMENTARY REPORT NUMBER AFSWC-TDR-63-49

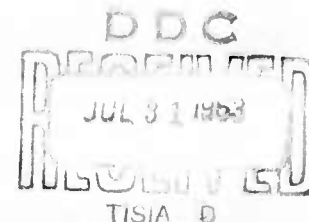


Research Directorate  
AIR FORCE SPECIAL WEAPONS CENTER  
Air Force Systems Command  
Kirtland Air Force Base  
New Mexico

This research has been funded by the  
Defense Atomic Support Agency

Project No. 5776, Task No. 577601

(Prepared under Contract AF 29(601)-5134  
by J. Roth, Stanford Research Institute,  
Poulter Laboratories, Menlo Park, Calif.)



HEADQUARTERS  
AIR FORCE SPECIAL WEAPONS CENTER  
Air Force Systems Command  
Kirtland Air Force Base  
New Mexico

When Government drawings, specifications, or other data are used for any purpose other than in connection with a definitely related Government procurement operation, the United States Government thereby incurs no responsibility nor any obligation whatsoever; and the fact that the Government may have formulated, furnished, or in any way supplied the said drawings, specifications, or other data, is not to be regarded by implication or otherwise as in any manner licensing the holder or any other person or corporation, or conveying any rights or permission to manufacture, use, or sell any patented invention that may in any way be related thereto.

This report is made available for study upon the understanding that the Government's proprietary interests in and relating thereto shall not be impaired. In case of apparent conflict between the Government's proprietary interests and those of others, notify the Staff Judge Advocate, Air Force Systems Command, Andrews AF Base, Washington 25, DC.

This report is published for the exchange and stimulation of ideas; it does not necessarily express the intent or policy of any higher headquarters.

Qualified requesters may obtain copies of this report from DDC. Orders will be expedited if placed through the librarian or other staff member designated to request and receive documents from DDC.

## FOREWORD

The writer gratefully acknowledges the contributions of the following members of Stanford Research Institute: Dr. Duvall for many helpful discussions and review of this report; Mr. Muller for help with some of the mathematics and for various interesting suggestions; Mr. Crosby for help in the phases of this study dealing with optics; Mr. Medlong for assembly and operation of the electronic gear; Mrs. Bain for computations; Mr. Rehbock for operating the streak camera; Mr. Mabus for help in shot assembly.

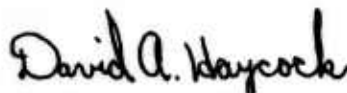
This report is further identified by the contractor's number SRI Project PGU-3997.

A B S T R A C T

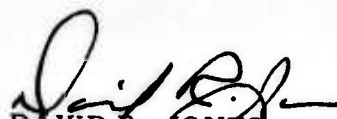
To fill a continued military demand for controlled explosive wave shaping this study has been undertaken to establish basic conditions for explosive systems capable of being initiated uniformly over their entire surface, and to demonstrate the functioning of the proposed system for simple geometries. This investigation is a continuation of that started under AFSWC TR-61-59. The proposed system consists of PVA lead azide initiated by radiation from an argon flash bomb. In addition to lead azide, the suggested explosive train consists of PETN and Comp B. Uniformity of initiation in this train is quite good, but can undoubtedly be improved if lead azide in sheet form becomes available. Because sheet azide was unavailable, the applicability of the proposed system has not been demonstrated for curved explosive surfaces, but it is believed that surface initiation of curved surfaces can be achieved.

PUBLICATION REVIEW

This report has been reviewed and is approved.



DAVID A. HAYCOCK  
Lt USAF  
Project Officer



DAVID R. JONES  
Colonel USAF  
Chief, Physics Branch



PERRY L. HUIE  
Colonel USAF  
Chief, Research Division

## CONTENTS

---

1. INTRODUCTION . . . . .	1
a. Objectives . . . . .	1
b. Previous Work. . . . .	1
c. Assessment of Present Investigation. . . . .	2
2. EXPERIMENTAL . . . . .	3
a. General Considerations . . . . .	3
b. Procedures and Apparatus . . . . .	4
(1) Lead Azide Assemblies . . . . .	4
(2) Windows and Filters . . . . .	5
(3) Argon Boxes . . . . .	5
(4) Argon . . . . .	7
(5) Plane-Wave Generators . . . . .	7
(6) Measurement of Initiation Delay . . . . .	7
(7) Measurement of Transit Times. . . . .	8
(8) Relative Light Intensity. . . . .	9
(9) Spectral Response of the Photomultiplier. . . . .	11
(10) Temperature and Radiation Distribution Measurements of Shocked Argon. . . . .	11
c. Results. . . . .	15
(1) Argon Shock Velocity. . . . .	15
(2) Azide Reflectivity. . . . .	15
(3) Azide Absorptivity. . . . .	15
(4) Relative and Effective Light Intensities. . . . .	18
(5) Transit Times . . . . .	21
(6) Initiation Delays . . . . .	21
(7) Normalization of Initiation Delays. . . . .	27
(8) Nature of Radiation of Shocked Argon. . . . .	28
(9) Temperature of Shocked Argon. . . . .	28
(10) Diameter Effect . . . . .	30
3. DISCUSSION . . . . .	33
a. Factors Influencing Initiation Delay Jitter. . . . .	33
(1) Incident Energy . . . . .	33
(2) Front-Surface Confinement and Particle Size . . . . .	33
(3) Effect of Azide Purity and Packing Density. . . . .	34
(4) Inherent Variability of Azide Assemblies. . . . .	36
(5) Summary . . . . .	36

# CONTENTS

b.	Dependence of Initiation Delay on Energy Absorption . . . . .	36
(1)	Model of the Initiation Process . . . . .	36
(2)	Calculation of $B_0$ . . . . .	38
(3)	Calculation of Radiant Energy Loss . . . . .	39
(4)	Calculation of $B$ for Black Boxes . . . . .	43
(5)	Constancy of $BT$ for Black Boxes . . . . .	43
(6)	Computation of $T_c$ for Mirror Boxes . . . . .	44
(7)	Independent Determination of $B_0$ . . . . .	45
(8)	Activation Energy of Lead Azide Decomposition . . . . .	48
(9)	Possibility of Photochemical Initiation . . . . .	49
c.	Miscellaneous Observations Which Are Consistent with the Proposed Mechanism . . . . .	53
d.	Light Signals from Detonating Lead Azide . . . . .	53
e.	Effect of Front-Surface Confinement . . . . .	54
4.	SURFACE INITIATION SYSTEMS . . . . .	56
a.	Plane Wave Demonstration . . . . .	56
b.	Possible Uses of the Flash-Bomb System for Plane Wave Generators . . . . .	59
c.	Initiation of Curved Surfaces . . . . .	60
d.	Lead Azide Sheet . . . . .	61
e.	Improved Front-Surface Confinement . . . . .	62
f.	Explosive Train . . . . .	62
g.	Flash Bomb . . . . .	63
h.	Recommendations for Further Study . . . . .	63
	REFERENCES . . . . .	65
	APPENDIX . . . . .	67
	DISTRIBUTION . . . . .	69



## ILLUSTRATIONS

---

Figure 1	Schematic Diagram of Lead Azide—Flash Bomb System. . . . .	3
Figure 2	Transmissivity of Windows and Filters. . . . .	6
Figure 3	Spectral Reflectivity of Mirror Box Walls. . . . .	7
Figure 4	Arrangement for Measuring Initiation Delay. . . . .	8
Figure 5	Typical Streak Camera Record of Lead Azide Initiated with an Argon Flash-Bomb. . . . .	9
Figure 6	Typical Photomultiplier Record of Radiation from an Argon Flash-Bomb—2 inch Black Box. . . . .	10
Figure 7	Spectral Response of Photomultiplier. . . . .	13
Figure 8	Streak Camera Record of Plane Shock in Argon—Comp B Driver. . . . .	16
Figure 9	Diffuse Reflectivity of PVA Lead Azide Aggregates. . . . .	16
Figure 10	Absorption Coefficients for PVA Lead Azide Aggregates. . . . .	17
Figure 11	Effective Light Intensity. . . . .	20
Figure 12	Diffuse Reflectivity of Streak Camera Slit Holder. . . . .	29
Figure 13	Effect of Azide Column Diameter on Initiation Delay. . . . .	32
Figure 14	Effect of Intimacy of Front-Surface Confinement on Initiation Delay of PVA Lead Azide. . . . .	34
Figure 15	Effect of Azide Particle Size on Its Initiation Delay. . . . .	35
Figure 16	Sketch of the Postulated Temperature-Time Profile for Initiation of Lead Azide by Radiation from a Flash-Bomb. . . . .	37
Figure 17	Fraction of Radiated Energy Reaching 4-inch x 4-inch Surface from a Radiator Steadily Advancing Towards the Surface (No Reflections). . . . .	41
Figure 18	Fraction of Energy Reaching a 4-inch x 4-inch Surface from a Radiator Steadily Advancing Towards the Surface (With Reflections). . . . .	42
Figure 19	Constancy of $B_T$ for Nonreflecting Argon Containers. . . . .	44
Figure 20	Spectral Transmissivity of Heated Crown Glass. . . . .	47
Figure 21	Solutions of the Heat Balance Equation (Eq. 18) for PVA Lead Azide with a Pyrex Glass Window. . . . .	50
Figure 22	Assembly for Plane Wave Demonstration Shot. . . . .	57
Figure 23	Still and Streak Camera Record of Plane Wave Demonstration Shot. . . . .	58

## TABLES

---

Table I	Lead Azide Properties . . . . .	4
Table II	Trends in Type of Observed Light Breakout from Rear Face of Lead Azide. . . . .	10
Table III	Percent Transmission of Interference Filters. . . . .	12
Table IV	Spectral Emissivity of Comp B Shock in Argon and Krypton . . . . .	19
Table V	Transit Times for 0.188 inch I.D. PVA Lead Azide. . . . .	21
Table VI	Lead Azide Initiation Delays. . . . .	22
Table VII	Normalized Initiation Delays of PVA Lead Azide. . . . .	27
Table VIII	Blackbody Distribution of a Comp B Shock in Argon . . . . .	28
Table IX	Measured Temperature of Comp B Shock in Argon . . . . .	31
Table IX	(a) Miscellaneous Temperature Measurements of Comp B Shocks in Argon. . . . .	31
Table X	Effect of Lead Azide Purity on Initiation Delay . . . . .	35
Table XI	Effect of Packing Density on PVA Lead Azide Initiation Delay. . . . .	35
Table XII	Fraction of Absorbed Energy in Selected Wavelength Regions . . . . .	39
Table XIII	Average Mirror Reflectivities for Normal Incidence. . . . .	43
Table XIV	Critical Temperature Rise for PVA Lead Azide. . . . .	45
Table XV	Activation Energy for Initiation of PVA Lead Azide. . . . .	51
Table XVI	Plane Wave Demonstration; Summary of Analysis of Shot 9022 . . . . .	59
Table XVII	Initiation Delay for PVA Lead Azide Assemblies Tilted Toward the Comp B . . . . .	61
Table XVIII	Initiation Delays for 90/10 PVA Lead Azide/Formvar Sheet. . . . .	62

## 1. INTRODUCTION

### a. OBJECTIVES

Explosive systems capable of being uniformly and simultaneously initiated over their entire surface are in demand for many ordnance developments and defense measures. Previous study under Contract No. AF 29(601)-2844<sup>1</sup> showed that metal azides, initiated by high-intensity light from an argon flash bomb, gave reproducible initiation delays and might be expected to form the basis of a practical system of surface initiation. The present investigation is designed to fill the gaps in basic information about the light initiation of metal azides (Task I) and to apply this and previous information to the development of practical surface-initiation systems (Task II).

### b. PREVIOUS WORK

The primary objective of the previous investigation<sup>1</sup> was to determine factors influencing variability in metal azide initiation delay. To achieve a practical surface initiation system, this variability must be kept small.

The main findings may be summarized as follows:

- (1) Ball-milled PVA lead azide shows less initiation delay variability (jitter) than silver azide which, in turn, has much less jitter than dextrinated lead azide.
- (2) Jitter is reduced by placing glass or quartz "windows" in close contact with the azide surface facing the flash-bomb.
- (3) Usually jitter is a fairly constant fraction of the initiation delay. To reduce absolute jitter, initiation delays should be kept small.
- (4) The product of the initiation delay times the rate of energy absorption of the irradiated surface is a constant.
- (5) The lead azide initiation process is thermal rather than photochemical.

#### C. ASSESSMENT OF PRESENT INVESTIGATION

It is believed that Task I, as defined above, is now essentially complete. Except for the filling in of a few details, the factors influencing initiation delay jitter have been established. A mechanism for the initiation process has been proposed which is in accord with almost all the experimental results. Consequently, sufficient background information appears to be available for the design of a practical surface initiation system. Progress in the design of a practical surface-initiation system was greatly hampered by the temporary unavailability of lead azide in the proper configuration--uniform "sheets." However, it was demonstrated that the suggested system will function quite effectively for plane geometry in an explosive train consisting of closely spaced assemblies, containing lead azide (facing the flash-bomb) on PETN, over Comp B. With the proper lead azide sheet it is certain that the above system will be much improved and it will also be possible to try to surface-initiate curved explosive surfaces.

## 2. EXPERIMENTAL

### a. GENERAL CONSIDERATIONS

The main objective of this study is the development of a practical system of surface initiation. The system under investigation consists of lead azide as the initiating explosive and the radiation from an argon flash-bomb as the energy source. To achieve the objective, the jitter in the lead azide initiation delay must be small. Many factors could influence the initiation delay and delay jitter. The most obvious is the amount and spectral region of the absorbed argon radiation. Other factors might be particle size, purity, packing density, and prior conditioning of the azide. Confinement of the azide layers absorbing radiation might also be important. Finally, to develop a practical system, an explosive train having no more jitter than the azide initiation must be designed and tested.

For a better understanding of the experiments to be described below, an idealized schematic presentation of the system investigated is shown in Figure 1.

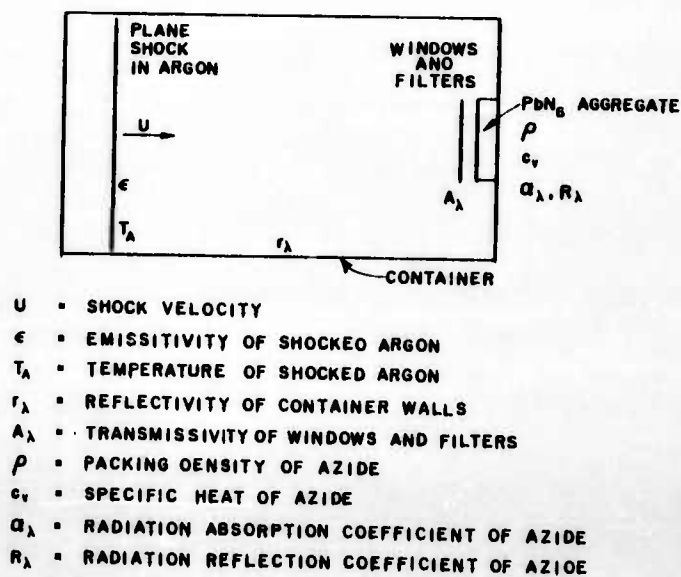


Figure 1 SCHEMATIC DIAGRAM OF LEAD AZIDE - FLASH BOMB SYSTEM

To study the effects of absorbed energy on initiation delay and delay jitter, one must measure the energy incident on the azide and determine what fraction of this energy is absorbed. This requires a knowledge of all the parameters listed in figure 1. The effects of confinement may be studied by changing the position and type of window. Prior conditioning of the azide presumably affects  $\alpha_\lambda$  and  $R_\lambda$ . Initiation delays can be conveniently determined by viewing the azide face opposite that which absorbs the radiation with a streak camera, and correcting for the transit time of an established detonation travelling through the azide assembly. Thus measurements of azide transit times have to be made for various loading densities, purity, and particle sizes.

#### b. PROCEDURES AND APPARATUS

##### (1) LEAD AZIDE ASSEMBLIES

The properties of the lead azides used in the present investigation are listed in Table I.

The azide was usually contained in nylon sleeves

which were normally 0.500-inch-O.D. and 0.188-inch-I.D. Occasionally steel sleeves of the same dimensions were used.

Confinement of the irradiated face was normally supplied by a window consisting of 1 cm-square portions of microscope

slides 39- to 40-mils thick of either Pyrex or crown glass, or of 64-mils-thick optical quartz. Some crown glass windows were only 10-mils thick. Usually windows were attached to empty sleeves with Pliobond cement and the azide was loaded into these assemblies at about 5000 psi by the Salinas Field Station of Unidynamics. In some instances azide was loaded into an assembly as described above, and then PETN, of about 80  $\mu$  particle size, was pressed on top of the azide. The PETN density ranged from 1.3 to 1.5 g/cc.

Table I  
LEAD AZIDE PROPERTIES

TYPE	PACKING DENSITY (g/cc)	PARTICLE SIZE ( $\mu$ )	PURITY
PVA	2.2-3.2	~0.5	Commercial; ball-milled
PVA	2.2-2.3	~0.5	Up to 15% organic impurity* deliberately introduced
Colloidal	2.5-2.6	~2	Very pure

\* Foravar.

As will become apparent, it is highly desirable to have lead azide in sheet form. Preliminary attempts to make uniform sheet azide were not too successful. Sheets up to 50-mils thick can be made by

premixing 90 parts of lead azide with 10 parts of Formvar (polyvinyl formal) dissolved in chloroform, and tumbling the slurry for several hours. The slurry is then poured into a form and the chloroform evaporated at room temperature. The resulting sheet is surprisingly tough but brittle. It is very porous having a density ranging from 1.3 to 1.6 g/cc. There appears to be some segregation of Formvar at the top and azide on the bottom of the sheet.

## (2) WINDOWS AND FILTERS

The optical transmissivity as a function of wavelength for various windows and filters used in this investigation is shown in figure 2. Transmissivities were determined on a Mod. 14 Carey Spectrophotometer. Filter supports, when used, were made as small as possible and placed relatively far from the azide column so as not to interfere with any radiation reflected from the argon container walls.

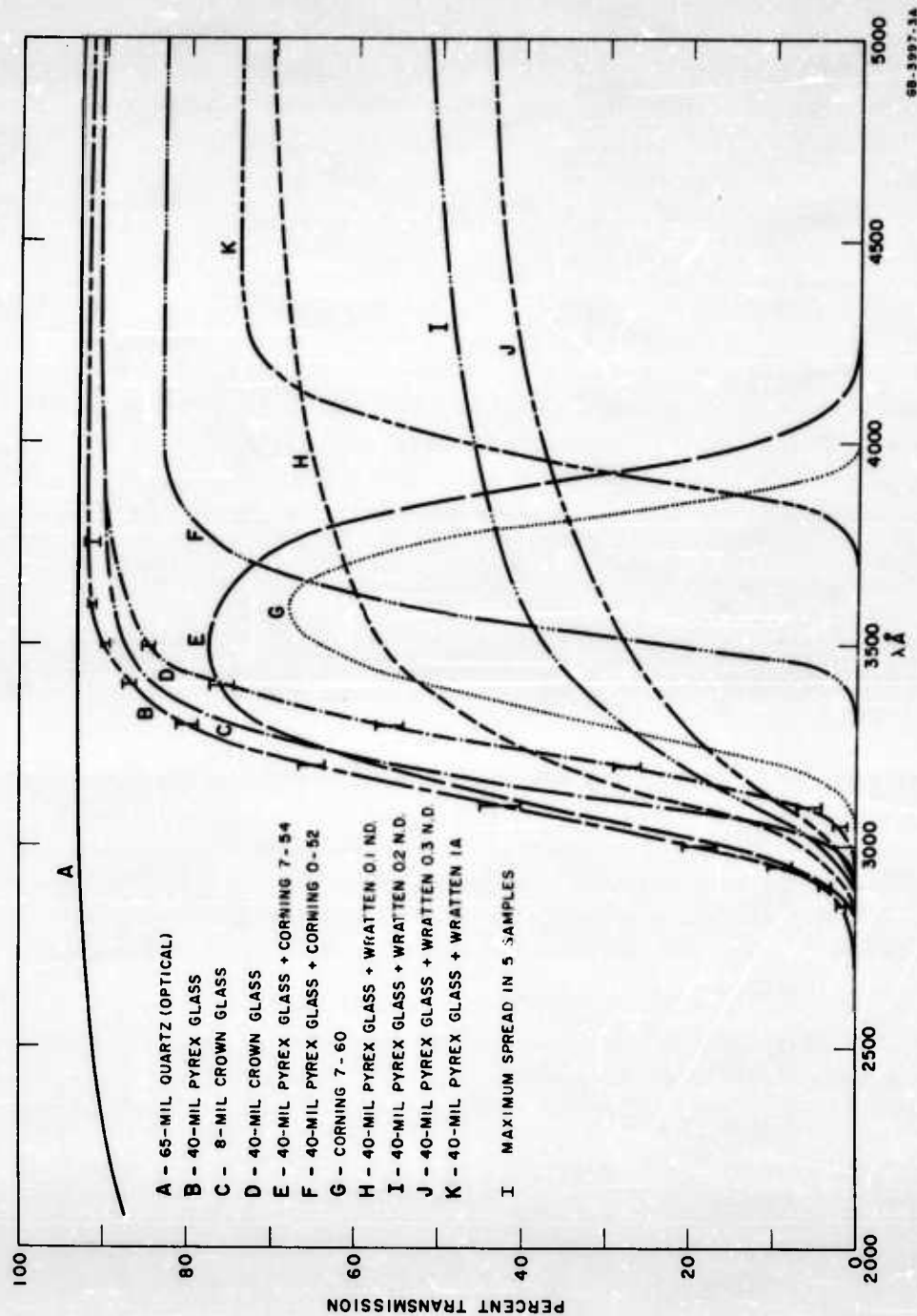
## (3) ARGON BOXES

In most instances the argon containers were open ended boxes made of front surface mirrors glued along their edges. A block of Comp B was taped to one open end, and a lucite holder containing the lead azide assemblies was taped to the other open end. A small copper tube was glued into a hole near the Comp B end to introduce the argon. The whole assembly was fairly gas tight. The cross section of the box was  $4 \times 4$  inches. Box length was either 8 or 4 inches. Mirrors were supplied by the Liberty Mirror Division, Libby-Owens-Ford Glass Company. Most mirrors were type 749 but in a few instances special ultraviolet reflecting mirrors were used. The reflectivity of the mirrors as measured by the manufacturer is shown in figure 3.

In three shots, the boxes were made of plywood with the insides painted a dull black.

In one shot, a mirror box (u.v. reflecting) was in the form of a frustum of a pyramid, tapering over a 4 inch length from  $4 \times 4$  inches at the azide end to  $2 \times 2$  inches at the comp B end.

For spectral distribution and temperature measurements of the argon flash  $\frac{1}{2}$ -inch-I.D. lucite tubes closed at one end with a lucite window were used (small scale shots).



68-3997-3A

Figure 2 TRANSMISSIVITY OF WINDOWS AND FILTERS



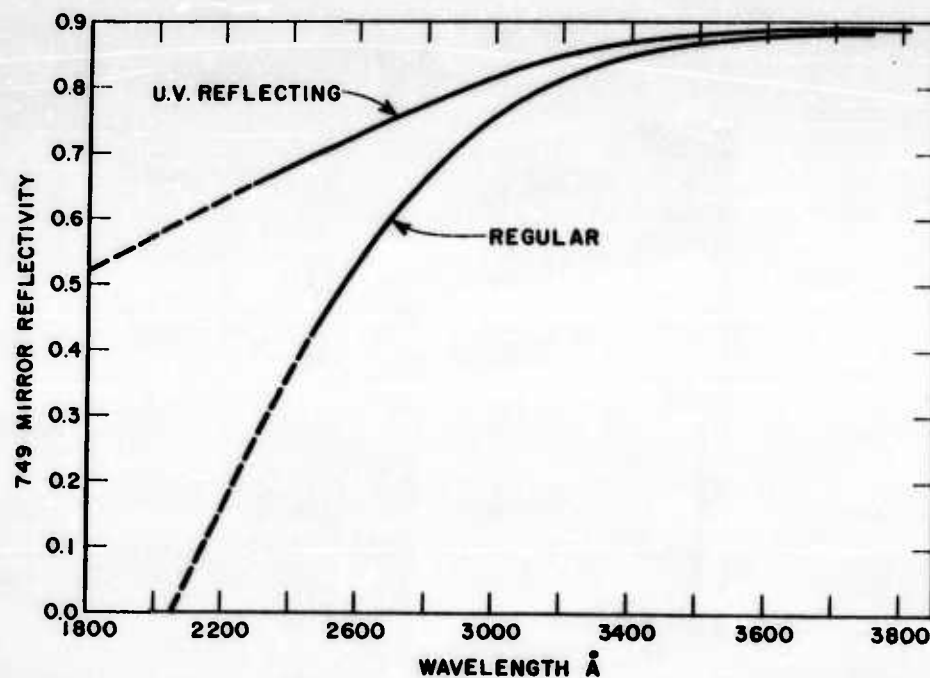


Figure 3 SPECTRAL REFLECTIVITY OF MIRROR BOX WALLS

(4) ARGON

Argon was obtained from the Linde Air Reduction Company. It was introduced through a copper tube about  $\frac{1}{8}$  inch from the bottom of the Comp B pad and issued through a  $\frac{1}{16}$ -inch hole near the upper corner of the lucite holder. Flow at 2 psi was started at least twenty minutes before the shot and continued during the shot.

(5) PLANE WAVE GENERATORS

In all shots, a  $4 \times 4 \times 2$ -inch pad of Comp B of 1.7 g/cc density was taped to the box in direct contact with the argon. This pad was plane wave initiated by either a 4-inch "Flower-pot"<sup>3</sup> or by a P-40.<sup>3</sup> The shock in argon was always plane to within a few shakes ( $0.01 \mu\text{sec}$ ).

(6) MEASUREMENT OF INITIATION DELAY

The use of a streak camera to measure initiating delays was previously<sup>1</sup> described. A photograph of the set up is shown in figure 4.

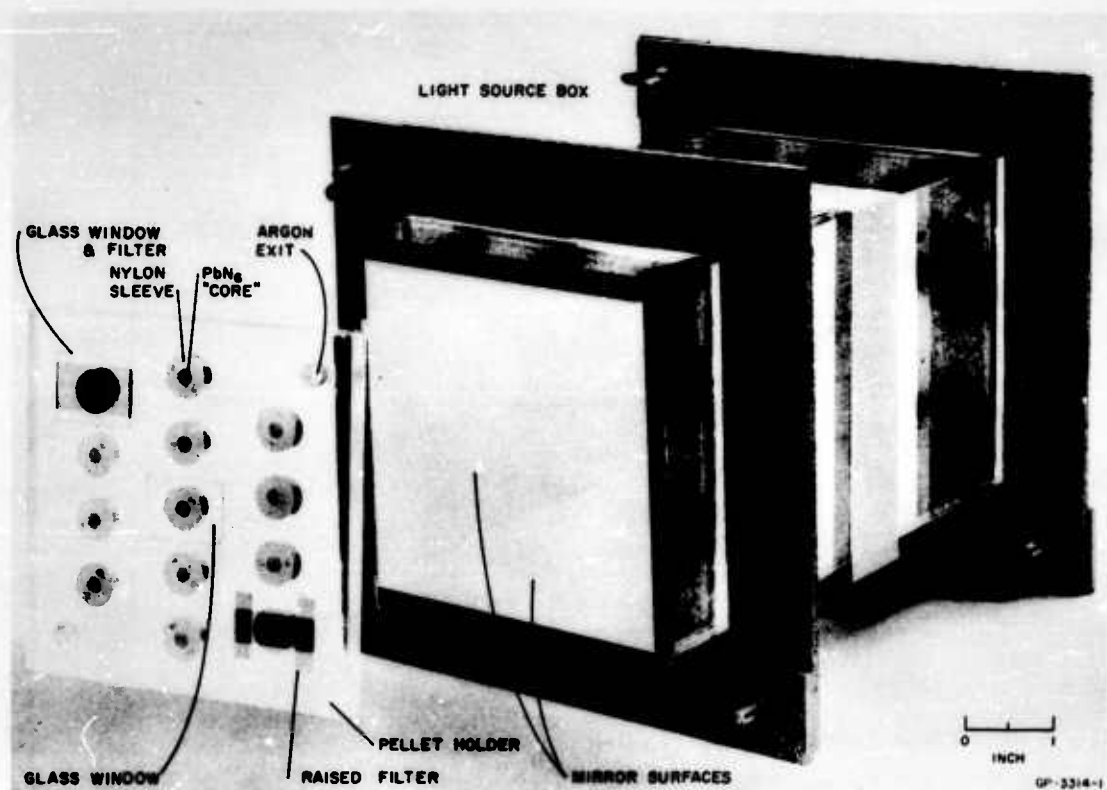


Figure 4 ARRANGEMENT FOR MEASURING INITIATION DELAYS

A typical record is shown in figure 5. Several different types of light breakout from the rear faces of lead azide assemblies have been observed (Fig. 5). Trends in the type of breakout are listed in Table II. A discussion of these trends follows in Sec. 3-d.

#### (7) MEASUREMENT OF TRANSIT TIMES

Time for a detonation to transverse a lead azide assembly (transit time) must be subtracted from the streak-camera time measurement (Fig. 5) to obtain initiation delays. The method of measuring transit times for an established detonation has been described.<sup>1</sup> It was found that the transit time through an azide assembly was the same whether it was initiated by Primacord or by styphnate-azide detonators.

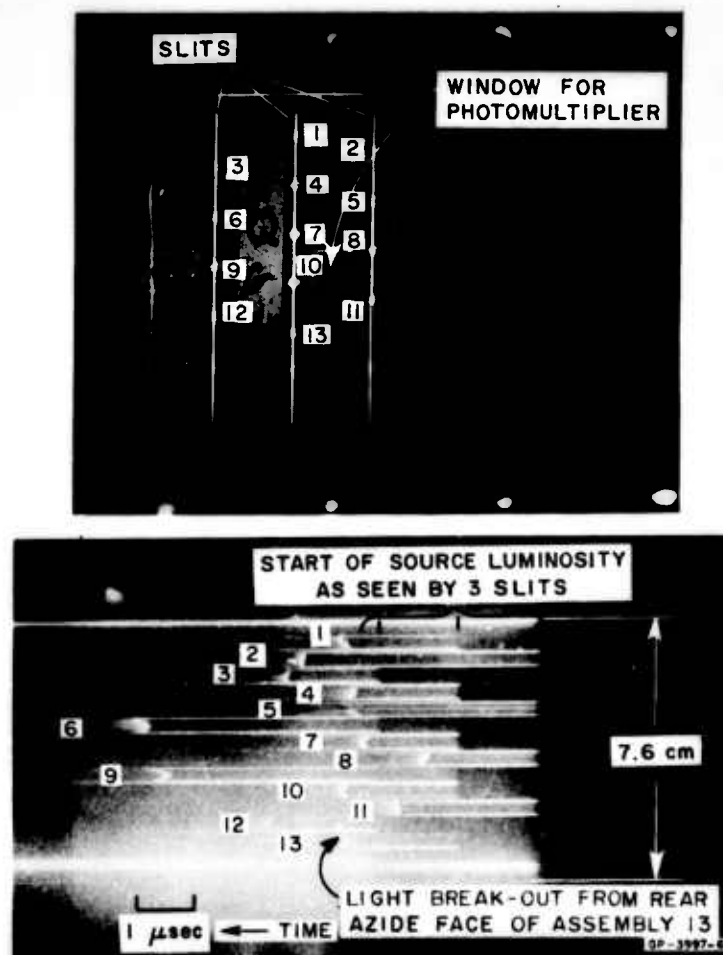


Figure 5 TYPICAL STREAK CAMERA RECORD OF LEAD AZIDE INITIATED WITH AN ARGON FLASH-BOMB

#### (8) RELATIVE LIGHT INTENSITY

A photomultiplier system (HCA 931) was used to obtain relative light intensity as previously described.<sup>1</sup> The photomultiplier outputs were recorded as voltage-time records on Tektronix Type 531 or 555 oscilloscopes. A typical record is shown in figure 6. Occasionally, interference filters, with back up filters to reduce second order transmissivity and decrease light intensity, were used to limit the spectral region of the light entering the photomultiplier.

Table II  
TRENDS IN TYPE OF OBSERVED LIGHT BREAKOUT  
FROM REAR FACE OF LEAD AZIDE

WINDOW	ARGON BOX LENGTH (inches)	AZIDE	BREAKOUT*	FREQUENCY
Pyrex	2 or 4	PVA	C or St.	13/19
Pyrex	4 or 8	Colloidal	C or St.	8/9
Pyrex	4 or 8	PVA/PETN composite*	St. or C	16/20
Pyrex	8	PVA pale	B, T or U	6/7
Pyrex	4 or 8	PVA/Formvar	St. or nearly St.	9/10
Quartz	4 or 8	PVA	S	8/10
Pyrex + O-52 Filter	4 or 8	PVA	C	4/5

\* C = (   
 St. = |   
 B = \   
 T = /   
 S = <   
 U = < or <

\* In this case the breakout is for PETN

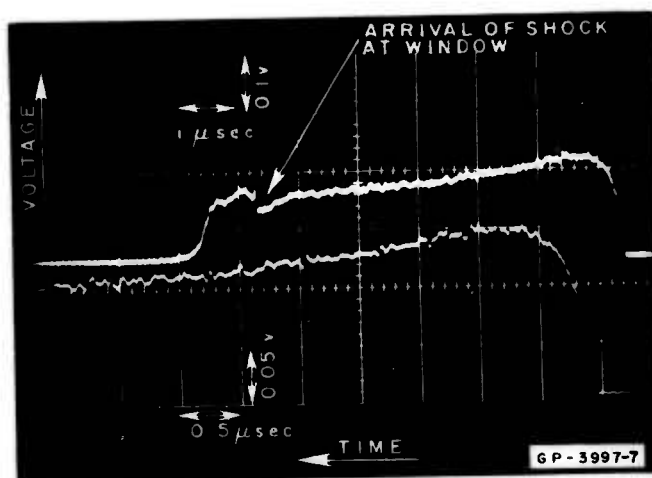


Figure 6 TYPICAL PHOTOMULTIPLIER  
RECORD OF RADIATION FROM  
AN ARGON FLASH-BOMB  
2-INCH BLACK BOX

#### (9) SPECTRAL RESPONSE OF THE PHOTOMULTIPLIER

Because the spectral response supplied by the manufacturer led to completely incoherent results, it became necessary to establish our own spectral response curve. Two N.B.S. calibrated tungsten lamps (500 watts and 100 watts) of 2854°K color temperature were used as energy sources. The photomultiplier was mounted on an optical bench exactly 1 meter from the tungsten lamp. The current to the lamp was carefully controlled to the values given in the N.B.S. calibration. Interference filters, with back-up filters to eliminate or minimize second-order transmissivity, were used. The spectral transmissivities of these filters, as measured on a Mod. 14 Carey Spectrophotometer, are given in Table III. The photomultiplier output was measured on a sensitive galvanometer. The data obtained were analyzed by the following procedure: If  $A_\lambda$  is the filter transmissivity at wavelength  $\lambda$ ,  $N_\lambda$  is the blackbody radiance at  $\lambda$  and  $T = 2854^\circ\text{K}$ , and  $P_\lambda$  is the spectral response of the photomultiplier then

$$\frac{\text{Output}}{\text{Output}'} = \frac{P_\lambda \int_{\lambda_1}^{\lambda_2} N_\lambda A_\lambda d\lambda}{P'_\lambda \int_{\lambda_3}^{\lambda_4} N'_\lambda A'_\lambda d\lambda} \quad (1)$$

where the primed quantities are for maximum observed output.  $P'_\lambda$  is taken to be unity, and the wavelength limits are determined by the filters used. Strictly speaking the  $P_\lambda$  should be under the integral sign, but for most of the regions of interest  $P_\lambda$  does not change rapidly with  $\lambda$  and the above method greatly simplifies the computation without introducing appreciable errors. The integrals were evaluated numerically from  $N_\lambda A_\lambda$  vs.  $\lambda$  plots, with  $N_\lambda$  obtained from blackbody tables.<sup>5</sup> The spectral response curve thus obtained for the photomultiplier used throughout this work is shown in figure 7. It was rechecked four months after the initial calibration and found to be essentially unchanged.

#### (10) TEMPERATURE AND RADIATION DISTRIBUTION MEASUREMENTS OF SHOCKED ARGON

As already mentioned,  $T_s$ , the temperature of shocked argon must be known to obtain the energy incident on the lead azide. One must also know how closely the radiation from shocked argon follows a blackbody

Table III

Wavelength microns	PICTURE FORCE*										BRIGHTNESS AND LOG									
	2	3	4	5	6	7	8	9	10	11	12	13	14	15	16	17	18	19	20	
1125	0.01	0.05	0.01	0.01	0.01	0.01	0.01	0.01	0.01	0.01	0.01	0.01	0.01	0.01	0.01	0.01	0.01	0.01	0.01	
1225	0.01	0.05	0.01	0.01	0.01	0.01	0.01	0.01	0.01	0.01	0.01	0.01	0.01	0.01	0.01	0.01	0.01	0.01	0.01	
1325	0.01	0.05	0.01	0.01	0.01	0.01	0.01	0.01	0.01	0.01	0.01	0.01	0.01	0.01	0.01	0.01	0.01	0.01	0.01	
1425	0.01	0.05	0.01	0.01	0.01	0.01	0.01	0.01	0.01	0.01	0.01	0.01	0.01	0.01	0.01	0.01	0.01	0.01	0.01	
1525	0.01	0.05	0.01	0.01	0.01	0.01	0.01	0.01	0.01	0.01	0.01	0.01	0.01	0.01	0.01	0.01	0.01	0.01	0.01	
1625	0.01	0.05	0.01	0.01	0.01	0.01	0.01	0.01	0.01	0.01	0.01	0.01	0.01	0.01	0.01	0.01	0.01	0.01	0.01	
1725	0.01	0.05	0.01	0.01	0.01	0.01	0.01	0.01	0.01	0.01	0.01	0.01	0.01	0.01	0.01	0.01	0.01	0.01	0.01	
1825	0.01	0.05	0.01	0.01	0.01	0.01	0.01	0.01	0.01	0.01	0.01	0.01	0.01	0.01	0.01	0.01	0.01	0.01	0.01	
1925	0.01	0.05	0.01	0.01	0.01	0.01	0.01	0.01	0.01	0.01	0.01	0.01	0.01	0.01	0.01	0.01	0.01	0.01	0.01	
2025	0.01	0.05	0.01	0.01	0.01	0.01	0.01	0.01	0.01	0.01	0.01	0.01	0.01	0.01	0.01	0.01	0.01	0.01	0.01	
2125	0.01	0.05	0.01	0.01	0.01	0.01	0.01	0.01	0.01	0.01	0.01	0.01	0.01	0.01	0.01	0.01	0.01	0.01	0.01	
2225	0.01	0.05	0.01	0.01	0.01	0.01	0.01	0.01	0.01	0.01	0.01	0.01	0.01	0.01	0.01	0.01	0.01	0.01	0.01	
2325	0.01	0.05	0.01	0.01	0.01	0.01	0.01	0.01	0.01	0.01	0.01	0.01	0.01	0.01	0.01	0.01	0.01	0.01	0.01	
2425	0.01	0.05	0.01	0.01	0.01	0.01	0.01	0.01	0.01	0.01	0.01	0.01	0.01	0.01	0.01	0.01	0.01	0.01	0.01	
2525	0.01	0.05	0.01	0.01	0.01	0.01	0.01	0.01	0.01	0.01	0.01	0.01	0.01	0.01	0.01	0.01	0.01	0.01	0.01	
2625	0.01	0.05	0.01	0.01	0.01	0.01	0.01	0.01	0.01	0.01	0.01	0.01	0.01	0.01	0.01	0.01	0.01	0.01	0.01	
2725	0.01	0.05	0.01	0.01	0.01	0.01	0.01	0.01	0.01	0.01	0.01	0.01	0.01	0.01	0.01	0.01	0.01	0.01	0.01	
2825	0.01	0.05	0.01	0.01	0.01	0.01	0.01	0.01	0.01	0.01	0.01	0.01	0.01	0.01	0.01	0.01	0.01	0.01	0.01	
2925	0.01	0.05	0.01	0.01	0.01	0.01	0.01	0.01	0.01	0.01	0.01	0.01	0.01	0.01	0.01	0.01	0.01	0.01	0.01	
3025	0.01	0.05	0.01	0.01	0.01	0.01	0.01	0.01	0.01	0.01	0.01	0.01	0.01	0.01	0.01	0.01	0.01	0.01	0.01	
3125	0.01	0.05	0.01	0.01	0.01	0.01	0.01	0.01	0.01	0.01	0.01	0.01	0.01	0.01	0.01	0.01	0.01	0.01	0.01	
3225	0.01	0.05	0.01	0.01	0.01	0.01	0.01	0.01	0.01	0.01	0.01	0.01	0.01	0.01	0.01	0.01	0.01	0.01	0.01	
3325	0.01	0.05	0.01	0.01	0.01	0.01	0.01	0.01	0.01	0.01	0.01	0.01	0.01	0.01	0.01	0.01	0.01	0.01	0.01	
3425	0.01	0.05	0.01	0.01	0.01	0.01	0.01	0.01	0.01	0.01	0.01	0.01	0.01	0.01	0.01	0.01	0.01	0.01	0.01	
3525	0.01	0.05	0.01	0.01	0.01	0.01	0.01	0.01	0.01	0.01	0.01	0.01	0.01	0.01	0.01	0.01	0.01	0.01	0.01	
3625	0.01	0.05	0.01	0.01	0.01	0.01	0.01	0.01	0.01	0.01	0.01	0.01	0.01	0.01	0.01	0.01	0.01	0.01	0.01	
3725	0.01	0.05	0.01	0.01	0.01	0.01	0.01	0.01	0.01	0.01	0.01	0.01	0.01	0.01	0.01	0.01	0.01	0.01	0.01	
3825	0.01	0.05	0.01	0.01	0.01	0.01	0.01	0.01	0.01	0.01	0.01	0.01	0.01	0.01	0.01	0.01	0.01	0.01	0.01	
3925	0.01	0.05	0.01	0.01	0.01	0.01	0.01	0.01	0.01	0.01	0.01	0.01	0.01	0.01	0.01	0.01	0.01	0.01	0.01	
4025	0.01	0.05	0.01	0.01	0.01	0.01	0.01	0.01	0.01	0.01	0.01	0.01	0.01	0.01	0.01	0.01	0.01	0.01	0.01	
4125	0.01	0.05	0.01	0.01	0.01	0.01	0.01	0.01	0.01	0.01	0.01	0.01	0.01	0.01	0.01	0.01	0.01	0.01	0.01	
4225	0.01	0.05	0.01	0.01	0.01	0.01	0.01	0.01	0.01	0.01	0.01	0.01	0.01	0.01	0.01	0.01	0.01	0.01	0.01	
4325	0.01	0.05	0.01	0.01	0.01	0.01	0.01	0.01	0.01	0.01	0.01	0.01	0.01	0.01	0.01	0.01	0.01	0.01	0.01	
4425	0.01	0.05	0.01	0.01	0.01	0.01	0.01	0.01	0.01	0.01	0.01	0.01	0.01	0.01	0.01	0.01	0.01	0.01	0.01	
4525	0.01	0.05	0.01	0.01	0.01	0.01	0.01	0.01	0.01	0.01	0.01	0.01	0.01	0.01	0.01	0.01	0.01	0.01	0.01	
4625	0.01	0.05	0.01	0.01	0.01	0.01	0.01	0.01	0.01	0.01	0.01	0.01	0.01	0.01	0.01	0.01	0.01	0.01	0.01	
4725	0.01	0.05	0.01	0.01	0.01	0.01	0.01	0.01	0.01	0.01	0.01	0.01	0.01	0.01	0.01	0.01	0.01	0.01	0.01	
4825	0.01	0.05	0.01	0.01	0.01	0.01	0.01	0.01	0.01	0.01	0.01	0.01	0.01	0.01	0.01	0.01	0.01	0.01	0.01	
4925	0.01	0.05	0.01	0.01	0.01	0.01	0.01	0.01	0.01	0.01	0.01	0.01	0.01	0.01	0.01	0.01	0.01	0.01	0.01	
5025	0.01	0.05	0.01	0.01	0.01	0.01	0.01	0.01	0.01	0.01	0.01	0.01	0.01	0.01	0.01	0.01	0.01	0.01	0.01	
5125	0.01	0.05	0.01	0.01	0.01	0.01	0.01	0.01	0.01	0.01	0.01	0.01	0.01	0.01	0.01	0.01	0.01	0.01	0.01	
5225	0.01	0.05	0.01	0.01	0.01	0.01	0.01	0.01	0.01	0.01	0.01	0.01	0.01	0.01	0.01	0.01	0.01	0.01	0.01	
5325	0.01	0.05	0.01	0.01	0.01	0.01	0.01	0.01	0.01	0.01	0.01	0.01	0.01	0.01	0.01	0.01	0.01	0.01	0.01	
5425	0.01	0.05	0.01	0.01	0.01	0.01	0.01	0.01	0.01	0.01	0.01	0.01	0.01	0.01	0.01	0.01	0.01	0.01	0.01	
5525	0.01	0.05	0.01	0.01	0.01	0.01	0.01	0.01	0.01	0.01	0.01	0.01	0.01	0.01	0.01	0.01	0.01	0.01	0.01	
5625	0.01	0.05	0.01	0.01	0.01	0.01	0.01	0.01	0.01	0.01	0.01	0.01	0.01	0.01	0.01	0.01	0.01	0.01	0.01	
5725	0.01	0.05	0.01	0.01	0.01	0.01	0.01	0.01	0.01	0.01	0.01	0.01	0.01	0.01	0.01	0.01	0.01	0.01	0.01	
5825	0.01	0.05	0.01	0.01	0.01	0.01	0.01	0.01	0.01	0.01	0.01	0.01	0.01	0.01	0.01	0.01	0.01	0.01	0.01	
5925	0.01	0.05	0.01	0.01	0.01	0.01	0.01	0.01	0.01	0.01	0.01	0.01	0.01	0.01	0.01	0.01	0.01	0.01	0.01	
6025	0.01	0.05	0.01	0.01	0.01	0.01	0.01	0.01	0.01	0.01	0.01	0.01	0.01	0.01	0.01	0.01	0.01	0.01	0.01	
6125	0.01	0.05	0.01	0.01	0.01	0.01	0.01	0.01	0.01	0.01	0.01	0.01	0.01	0.01	0.01	0.01	0.01	0.01	0.01	
6225	0.01	0.05	0.01	0.01	0.01	0.01	0.01	0.01	0.01	0.01	0.01	0.01	0.01	0.01	0.01	0.01	0.01	0.01	0.01	
6325	0.01	0.05	0.01	0.01	0.01	0.01	0.01	0.01	0.01	0.01	0.01	0.01	0.01	0.01	0.01	0.01	0.01	0.01	0.01	
6425	0.01	0.05	0.01	0.01	0.01	0.01	0.01	0.01	0.01	0.01	0.01	0.01	0.01	0.01	0.01	0.01	0.01	0.01	0.01	
6525	0.01	0.05	0.01	0.01	0.01	0.01	0.01	0.01	0.01	0.01	0.01	0.01	0.01	0.01	0.01	0.01	0.01	0.01	0.01	
6625	0.01	0.05	0.01	0.01	0.01	0.01	0.01	0.01	0.01	0.01	0.01	0.01	0.01	0.01	0.01	0.01	0.01	0.01	0.01	
6725	0.01	0.05	0.01	0.01	0.01	0.01	0.01	0.01	0.01	0.01	0.01	0.01	0.01	0.01	0.01	0.01	0.01	0.01	0.01	
6825	0.01	0.05	0.01	0.01	0.01	0.01	0.01	0.01	0.01	0.01	0.01	0.01	0.01	0.01	0.01	0.01	0.01	0.01	0.01	
6925	0.01	0.05	0.01	0.01	0.01	0.01	0.01	0.01	0.01	0.01	0.01	0.01	0.01	0.01	0.01	0.01	0.01	0.01	0.01	
7025	0.01	0.05	0.01	0.01	0.01	0.01	0.01	0.01	0.01	0.01	0.01	0.01	0.01	0.01	0.01	0.01	0.01	0.01	0.01	
7125	0.01	0.05	0.01	0.01	0.01	0.01	0.01	0.01	0.01	0.01	0.01	0.01	0.01	0.01	0.01	0.01	0.01	0.01	0.01	
7225	0.01	0.05	0.01	0.01	0.01	0.01	0.01	0.01	0.01	0.01	0.01	0.01	0.01	0.01	0.01	0.01	0.01	0.01	0.01	
7325	0.01	0.05	0.01	0.01	0.01	0.01	0.01	0.01	0.01	0.01	0.01	0.01	0.01	0.01	0.01	0.01	0.01	0.01	0.01	
7425	0.01	0.05	0.01	0.01	0.01	0.01	0.01	0.01	0.01	0.01	0.01	0.01	0.01	0.01	0.01	0.01	0.01	0.01	0.01	
7525	0.01	0.05	0.01	0.01	0.01	0.01	0.01	0.01	0.01	0.01	0.01	0.01	0.01	0.01	0.01	0.01	0.01	0.01	0.01	
7625	0.01	0.05	0.01	0.01	0.01	0.01	0.01	0.01	0.01	0.01	0.01	0.01	0.01	0.01	0.01	0.01	0.01	0.01	0.01	
7725	0.01	0.05	0.01	0.01	0.01	0.01														

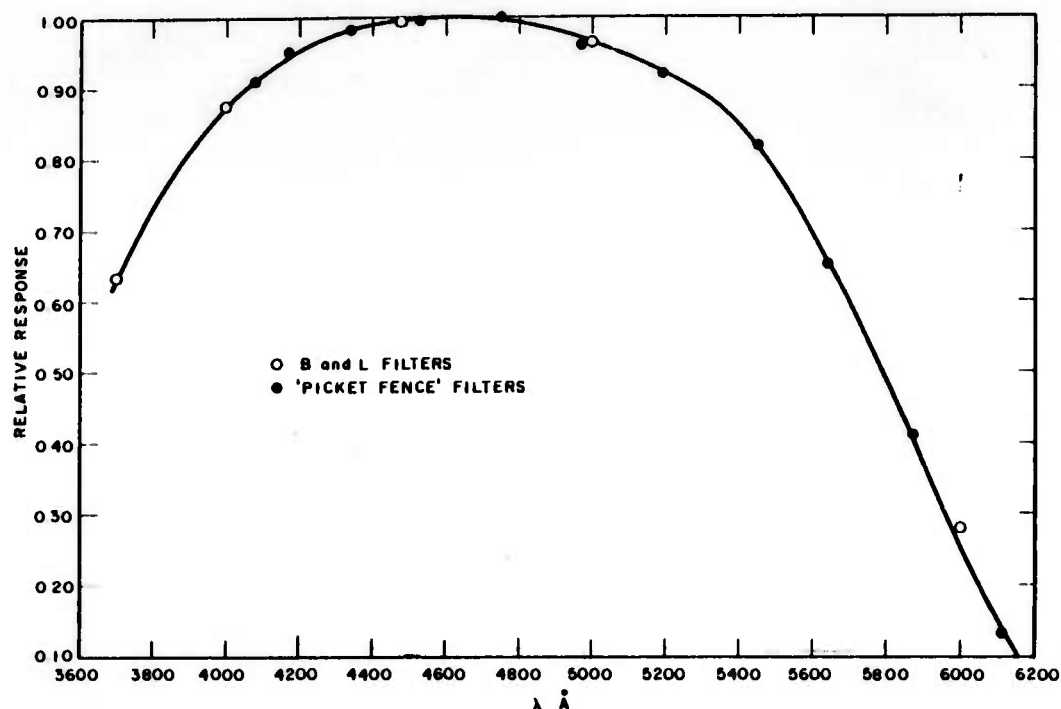


Figure 7 SPECTRAL RESPONSE OF PHOTOMULTIPLIER

distribution. The distribution can be obtained by viewing the radiation generated by a plane shock in argon with the photomultiplier system just described.

For this system

$$\frac{\text{Output}'''}{\text{Output}''} = \frac{\epsilon_{\lambda}'' \int_{\lambda_1}^{\lambda_2} N_{\lambda}''' A_{\lambda}''' P_{\lambda}''' d\lambda}{\epsilon_{\lambda}'' \int_{\lambda_3}^{\lambda_4} N_{\lambda}'' A_{\lambda}'' P_{\lambda}'' d\lambda} \quad (2)$$

Here the  $N_{\lambda}$ 's are for a fixed temperature but varying  $\lambda$ . The primes are used to distinguish different filter systems.

As will be shown later, the emissivities  $\epsilon_{\lambda}$  are all very close to unity and can therefore be taken outside the integral. In the expected temperature range the ratios of the integrals vary only very slowly with

$T_a$ . This is fortunate in studying energy distribution, but it means that Eq. (2) cannot be used to obtain  $T_a$ . To get  $T_a$  some standard source must be used in the same optical system and  $T_a$  evaluated by successive approximations of

$$\frac{\text{Output}}{\text{Output}'} = \frac{\epsilon_{\lambda} \int_{\lambda_1}^{\lambda_2} N_{\lambda} A_{\lambda} P_{\lambda} d\lambda}{\epsilon'_{\lambda} \int_{\lambda_1}^{\lambda_2} N'_{\lambda} A_{\lambda} P_{\lambda} d\lambda} \quad (3)$$

where the primed quantities are for the standard source and output ratios are for the same filter.

Most of the distribution and all temperature measurements were made in a scaled-down system using a special plane wave generator<sup>22</sup> to initiate 0.5-inch-diameter, 1-inch-long Comp B rods contained in argon filled, 0.5-inch-I.D., 3-inch-long, lucite tubes closed at one end with 1/6-inch lucite (lucite is transparent down to 3500 Å). A 0.27-inch-circular diaphragm was positioned over the center of this lucite end piece to cut out extraneous light. The center of the Comp B rod was carefully aligned with the photo cathode and the interference filters were positioned as close to it as feasible. A 10-inch-focal-length lens was used to focus the shot light on the photo cathode. The optical path lengths were: shot container end piece to a protective window, 18.5 inches; protective window to focusing lens, 14.5 inches; lens to photo cathode; 18.5 inches. Since a portion of the protective window had to be replaced after every shot, several Xe flasher<sup>1</sup> outputs were recorded before each shot. Because the Xe flasher output was found to be constant to within 3 percent, it was possible by this procedure to have a continuous check on the constancy of the optical system and to correct for the minor changes which occurred. The photomultiplier outputs were recorded as voltage-time traces on Tektronix Type 531 and 555 oscilloscopes.

The standard source for the temperature measurements was a tungsten ribbon lamp operated at 7.59 amps. It was carefully aligned so that the position of the central portion of the ribbon corresponded very closely to that of the center of the Comp B rods. Its temperature was measured by optical pyrometers and by using its output ratios in Eq. (2).\*

\* For temperatures in the range of a few thousand °K,  $N_{\lambda}$  is very sensitive to temperature, and Eq. (2) can be used to determine distribution as well as temperature.



In an effort to shorten light intensity rise timea (Fig. 6); thin discs of various materials were placed on the Comp B face exposed to the argon. For the same reason, in one of the lucite shota, the lucite tube was flushed with argon and then filled with krypton.

### c. RESULTS

#### (1) ARGON SHOCK VELOCITY

A streak camera record of a plane wave initiated Comp B shock in argon in a 4 x 4 x 8-inch plywood box is shown in figure 8. The implications of the fainter luminosity ahead of the main bright shock are discussed in the Appendix. The main shock propagates at a steady velocity of  $8.3 \pm 0.1$  mm/ $\mu$ sec for at least 10 cm from the Comp B face. An average shock velocity of 8.3 mm/ $\mu$ sec can also be obtained from a relative light intensity record like that in figure 6.

#### (2) AZIDE REFLECTIVITY

No new measurements were made on azide reflectivity. Diffuse reflectivity data were taken from previous work.<sup>1</sup> For the convenience of the reader the  $R_\lambda$  vs.  $\lambda$  curves are reproduced in figure 9.

#### (3) AZIDE ABSORPTIVITY

The techniques for measuring azide absorption coefficients are described in Ref. 1. In the previous work<sup>1</sup> insufficient attention was paid to density variations in the azide aggregatea for which light transmission was meaured. Better density and thickneaa control in the present series of measurements resulted in somewhat different absorption coefficients than previously reported. The new absorption coefficients,  $\alpha_\lambda$ , are given in figure 10. They were calculated from meaured transmissivities according to the relation

$$\alpha_\lambda = \frac{2.3}{\rho h} [\log (I_0/I_T)_\lambda + \log (1 - R_\lambda)] \quad (4)$$

where  $\rho$  and  $h$  are azide aggregate density and thickness,  $I_0$  is the incident light intensity,  $I_T$  is the transmitted light intensity, and  $R_\lambda$  is the reflectivity.

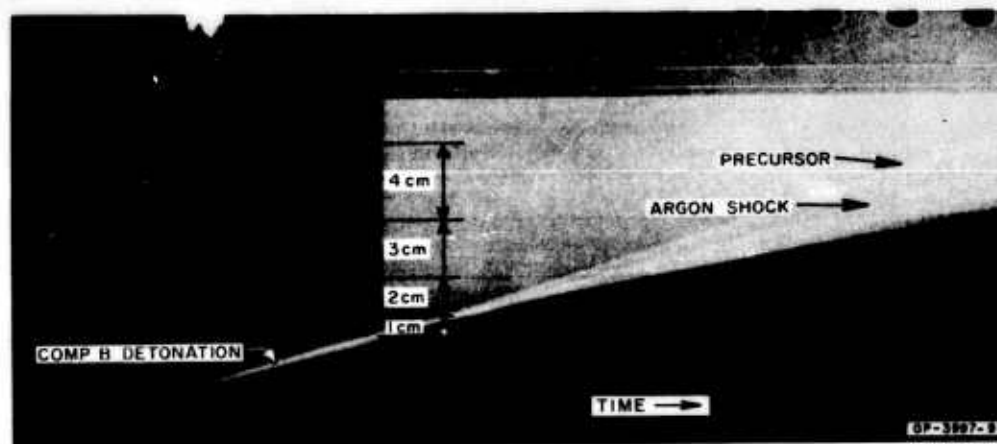


Figure 8 STREAK CAMERA RECORD OF PLANE SHOCK  
IN ARGON - COMP B DRIVER

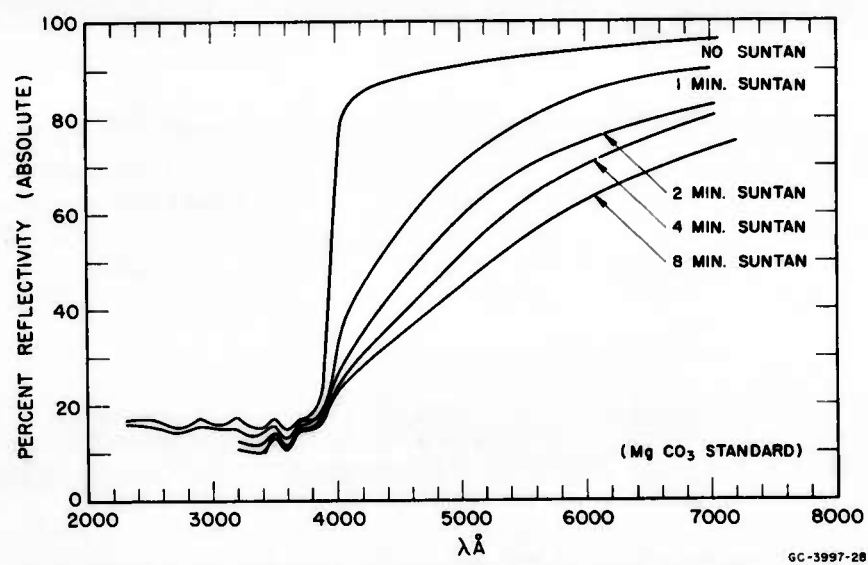
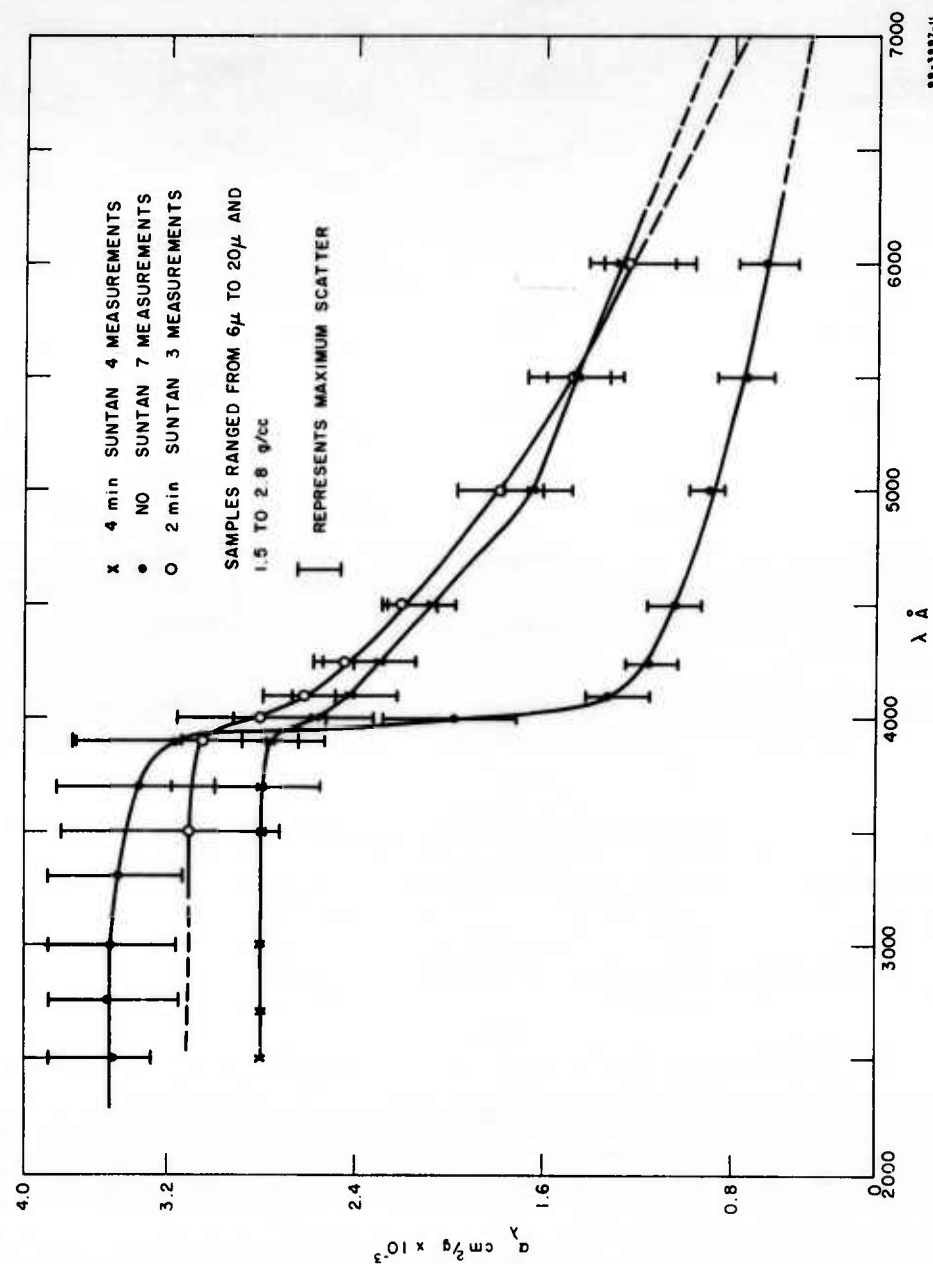


Figure 9 DIFFUSE REFLECTIVITY OF PVA LEAD AZIDE AGGREGATES



99-3397-II

Figure 10 ABSORPTION COEFFICIENTS FOR PVA LEAD AZIDE AGGREGATES

#### (4) RELATIVE AND EFFECTIVE LIGHT INTENSITIES

All photomultiplier records of argon flash-bomb radiation show definite rise times to peak light intensity (Fig. 6). It has been shown that this rise time is not caused by the electronica in the photomultiplier system nor should it be caused by the very short times required to reach ionization equilibrium (Appendix B).


The correct explanation of the long rise times is believed to be as follows: Immediately after the Comp B shock enters the argon, the shocked layer is very thin. If the thin argon layer is relatively transparent, its emissivity is low and consequently the photomultiplier records a low light intensity. As the shock advances, the shocked argon layer gets thicker and more opaque and its emissivity increases. On this basis the maximum in the relative light intensity-time curve corresponds to radiation from a sufficiently thick argon layer to have essentially complete opacity. Thereafter the radiation intensity could decrease because of (1) rarefactions, or (2) absorption of visible radiation (this is the only type arriving at the photo cathode) by unshocked argon which has been heated by u.v. radiation from the shocked argon. The steadiness of the measured shock velocity in the regular shots ( $4 \times 4$ -inch cross section) argues against the first reason. Zeldovich<sup>6</sup> has presented arguments in support of the second. Also in support are some preliminary time-resolving spectrograph records made in this laboratory. Argon absorption lines in the visible region were found superimposed on the continuous radiation. These lines appeared about  $3 \mu\text{sec}$  after the Comp B shock entered the argon. This may be the heat-up time of the unshocked argon. In any event, 2 to  $3 \mu\text{sec}$  is about the time found for noticeable decrease of the relative light intensity.

If the proposed explanation of the rise time is correct, then at any time,  $t$ , for shocked argon of thickness  $x$ , and absorption coefficient  $\alpha$ ,

$$I_{rel} = \frac{\epsilon_t}{\epsilon_{max}} = \frac{1 - e^{-\alpha x}}{1 - e^{-\alpha x_{max}}} = \frac{1 - e^{-\alpha U t}}{1 - e^{-\alpha U t_{max}}} \quad (5)$$

since the shock advances at a steady velocity  $U$ . (The quantities labelled "max" are for peak light intensity.) Equation (5) can be solved by successive approximations to give the values of  $\alpha$  and  $\epsilon$  listed in Table IV.

Table IV  
SPECTRAL EMISSIVITY OF COMP B SHOCK IN ARGON AND KRYPTON

FILTERS	SHOTS <sup>a</sup>	AVG $t_{\max}$ ( $\mu\text{sec}$ )	RANGE ( $\mu\text{sec}$ )	AVG $\alpha^{\dagger}$ ( $\text{cm}^{-1}$ )	RANGE ( $\text{cm}^{-1}$ )	AVG $\epsilon_{\text{max}}^{\S}$	COMP B COVER
B & L 600 + Wratten No. 8	2 <sup>o</sup>	0.615	0.60-0.63	8.8	7.8-9.8	0.982	none
B & L 500 + Wratten 1 A	3 <sup>o</sup>	0.66	0.65-0.68	7.4	6.8-7.8	0.982	<div style="text-align: center;">  </div>
B & L 450 + Wratten 1 A	5	0.72	0.70-0.75	6.2	5.2-6.6	0.976	
B & L 400 + Wratten 1 A	2	0.81	0.77-0.85	5.1	4.6-5.3	0.967	
B & L 400 + Wratten 1 A	2	0.715	0.70-0.73	6.1	5.4-7.0	0.973	
Kodak 18 A <sup>c</sup>	3	0.73	0.72-0.76	8.0	6.8-10.0	0.992	
B & L 450 + Wratten 1 A	1 <sup>a</sup>	1.35	--	1.7	1.6-1.8	0.900	
B & L 450 + Wratten 1 A	1 <sup>o</sup>	0.70	--	7.6	7.4-8.1	0.988	
B & L 450 + Wratten 1 A	1 <sup>o</sup>	0.75	--	6.5	5.8-7.0	0.983	
B & L 450 + Wratten 1 A	1 <sup>a</sup>	0.46	--	10.1 <sup>b</sup>	9.9-10.4	0.979	5-mil aluminized Mylar 1-mil Al diac none; Kr gas

<sup>a</sup> At least 5 measurements per shot.

<sup>†</sup>  $\alpha = \frac{2.3}{U\tau} \log(1 - \epsilon_{\max} I_{\text{rel}})$ ; solved by successive approximations using  $U = 8.3 \text{ mm}/\mu\text{sec}$ .

<sup>§</sup>  $\epsilon_{\max} = 1 - e^{-\alpha U \tau}$ ; solved by successive approximations using  $U = 8.3 \text{ mm}/\mu\text{sec}$ .

<sup>a</sup> Small-Scale Shots only.

<sup>b</sup> Assuming  $U = 8.3 \text{ mm}/\mu\text{sec}$ .

<sup>c</sup> Max. Transmission at around 3600 to 3700 Å.

Note that  $\epsilon_{\max}$  is very close to unity, which agrees with the measurements (about to be discussed) showing that argon flash-bomb radiation is black-body.

A following section will show that many initiation delays are of the same magnitude as the relative intensity rise times. Consequently any comparisons based on radiant energy flux must be corrected to take rise times into account. To do this conveniently an effective relative light intensity  $\bar{I}$  is defined as

$$\bar{I} = \frac{\int_0^{\tau} I dt}{\tau} \quad (6)$$

where  $\tau$  is the observed initiation delay. Plots of  $\bar{I}$  vs.  $\tau$  are given in figure 11 for white light,  $4500 \text{ Å} \pm 80 \text{ Å}$ ,  $4000 \text{ Å} \pm 90 \text{ Å}$ , and approximately  $3700 \text{ Å} \pm 400 \text{ Å}$  light. The deviations are half widths of the filters used with the photomultiplier. Fortunately, most of the observed  $\tau$ 's place  $\bar{I}$  in the relatively flat regions of the  $\bar{I}$  vs.  $\tau$  curves.

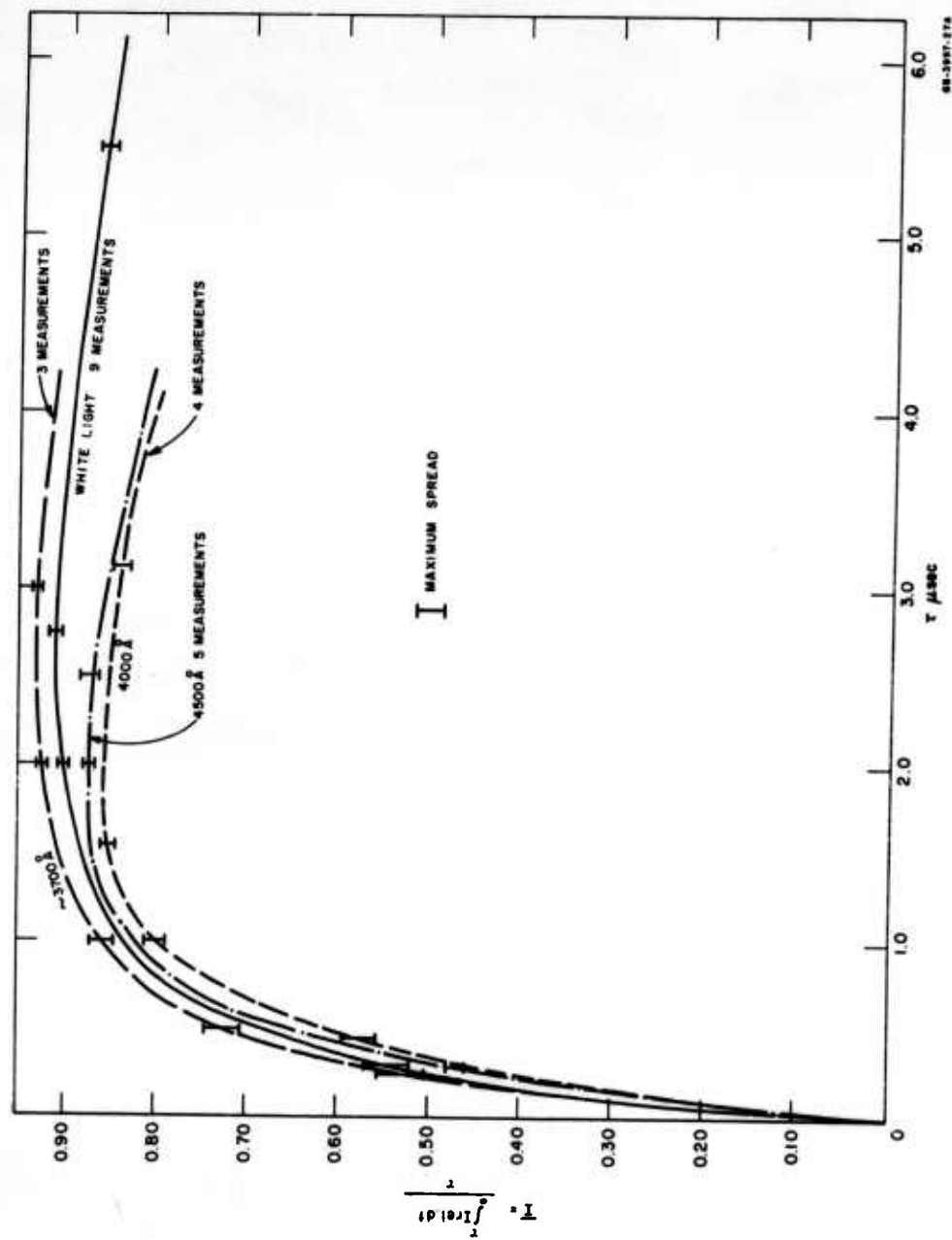


Figure 11 EFFECTIVE LIGHT INTENSITY

### (5) TRANSIT TIMES

Times for an established detonation to traverse various lead azide and lead azide-PETN assemblies are given in Table V. The previously determined<sup>1</sup> average transit time for 0.100 in high PVA lead azide was 0.80  $\mu$ sec. There appears to be no correlation between azide density scatter and transit time scatter.

Table V  
TRANSIT TIMES FOR 0.188 inch I.D. PVA LEAD AZIDE

NO. OF MEASUREMENTS	DENSITY (g/cc)		EXPLOSIVE HEIGHT (inches)		SLEEVE MATERIAL (0.500 in. O.D.)	TOTAL TRANSIT TIME ( $\mu$ /sec)	AZIDE DETONATION VELOCITY (mm/ $\mu$ sec)
	Azide	PETN	Azide	PETN			
12	2.27 (2.18-2.42) <sup>a</sup>	--	0.101 (0.100-0.103)	--	Nylon	0.82 (0.78-0.88)	3.1
2	2.2 (--)	--	0.200 (--)	--	Steel	1.69 (1.66-1.72)	3.0
5	2.99 (2.92-3.06)	1.34 (1.33-1.36)	0.044 (0.43-0.45)	0.0156 (0.154-0.159) <sup>a</sup>	Steel	0.90 (0.88-0.93) <sup>c</sup>	3.5 <sup>c</sup>
3	3.14 (3.10-3.20)	1.57 (1.57-1.59)	0.057 (0.055-0.058)	0.144 (0.143-0.146) <sup>b</sup>	Nylon	0.99 (0.99-1.00) <sup>b</sup>	2.8 <sup>c</sup> 3.5 <sup>c,d</sup>

<sup>a</sup> Numbers in parentheses give range of variation. Preceding number is the mean value.

<sup>a</sup> PETN was about 80  $\mu$ .

<sup>b</sup> PETN was about 250  $\mu$ .

<sup>c</sup> PETN was assumed to detonate at a velocity depending on packing density as given by Conk.<sup>4</sup>

<sup>d</sup> Assuming 0.1  $\mu$ sec delay in initiating the "coarse" PETN.

### (6) INITIATION DELAYS

All the initiation delays measured during this investigation and the conditions of measurements are listed in Table VI. As previously discussed,<sup>1</sup> suntanning of the azide appears to reduce initiation delay jitter. Therefore, all assemblies were exposed to noon sunlight for four minutes—suntanned—on the day before the shot. Exposure was through the window on an assembly. Filters, if used, were placed over the windows after suntanning. Whenever available (as it was for most shots) the ratio of the effective peak photomultiplier output, to the average of the three highest observed effective peak outputs is shown in Table VI. Factors influencing peak intensity are discussed in Sec. 4-g. It is felt that the average of three highest observed intensities represents the energy flux of an argon flash-bomb under optimum conditions. The various factors influencing initiation delay will be considered separately later on.

Table VI  
LEAD AZIDE INITIATION DELAYS

SHOT NO.	AZIDE	DENSITY (g/cc)	CONFINEMENT	MIRRORBOX LENGTH (inches)	FILTER	LIGHT BREAK-OUT†	RELATIVE INTENSITY I%	INITIATION DELAY Δ (μsec)	AVG DELAY (μsec)	REMARKS
8580 ↓	PVA ↓	~2.2 ↓	Pyrex ↓	8 ↓	none ↓	C T S T C U S C T T C C	-- -- -- -- -- -- -- -- -- -- -- -- --	0.96 1.10 1.31? 0.99 1.16 0.98 1.06 0.97 1.26 1.27 1.00 1.00	1.03           1.27 1.00	           at 30° from vertical at 30° from vertical at 22° from vertical at 22° from vertical
8576 <sup>a</sup> ↓	PVA ↓	~2.2 ↓	Pyrex ↓	8 ↓	none ↓	B T S S C C	-- -- -- -- -- --	0.97 1.01 0.95 1.07 1.04 0.96	1.00	
8581 <sup>b</sup> ↓	PVA ↓	~2.2 ↓	Pyrex ↓	8 ↓	none ↓	T C S M C C U S S C T S T	0.84 <sup>b</sup> ↓	1.08 1.00 1.02 1.08 0.93 1.08 1.16 1.00 1.06 1.06 1.12 0.98 1.07	1.05	
8584 ↓	PVA ↓	2.20 ± 0.05 ↓	Pyrex ↓	8 ↓	none ↓	S M M M U T M C S S S	0.68 ↓	1.24 1.37 1.30 1.27 1.26 1.32 1.31 1.23 1.26 1.24 1.31	1.29	
8590 <sup>c</sup> ↓	PVA ↓	~2.2 ↓	Crown ↓	8 ↓	none ↓	S B B H S T S S S S B	0.855 ↓	1.16 1.20 1.38 1.44 1.51 1.45 1.28 1.19 1.32 1.12 1.18 1.12	1.18 1.43     1.26   1.14	no suntan; 10°C no suntan; 10°C no suntan; 10°C no suntan; 10°C no suntan; 140°C no suntan; 140°C no suntan; 140°C no suntan; 220°C no suntan; 220°C no suntan; 220°C
8679 ↓	PVA ↓	2.40 ± 0.05 ↓	Pyrex Pyrex Crown Crown ↓	8 ↓	none ↓	M S T S M	0.93 ↓	0.33 0.97 1.08 1.13 1.09	0.93 1.10	



Table VI continued

SHOT NO.	AZIDE	DENSITY (g/cc)	CONFINEMENT	MIRRORBOX LENGTH (inches)	FILTER	LIGHT BREAK-OUT†	RELATIVE INTENSITY I/S	INITIATION DELAY Δ (μsec)	AVG DELAY (μsec)	REMARKS
8680 ↓	PVA ↓	2.40 ± 0.05 ↓	Pyrex ↓	8 ↓	none ↓	B C T S S St	0.81 ↓	1.10 0.99 1.10 1.12 1.06 1.14	1.08	
8681 ↓	PVA ↓	2.40 ± 0.05	Pyrex Pyrex Pyrex Pyrex Crown Crown	8 ↓	none ↓	M C T T S B	~0.81 ↓	7.05 6.74 6.88 6.82 8.47 8.60	6.88 8.53	Black box ↓
8720 ↓	PVA ↓	2.40 ± 0.05 ↓	Pyrex Pyrex Pyrex Crown Crown	8 ↓	none ↓	B C C C C	1.00 ↓	0.93 0.86 0.83 1.00 0.90	0.87 0.95	10-mil confinement 10-mil confinement
8719 ↓	PVA PVA PVA PVA/PETN <sup>c</sup> ↓ PVA/PETN <sup>d</sup> ↓	2.40 ± 0.05 2.40 ± 0.05 2.40 ± 0.05 3.14 ± 0.08/ 1.52 ± 0.02 ↓ 3.05 ± 0.10/ 1.42 ± 0.02 ↓	Pyrex ↓	8 ↓	none ↓	U C U C  C C C C St St	0.975 ↓	0.85 0.89 0.89 1.09  0.96 0.92 1.00 0.84  0.88 0.90	0.88 0.99 0.87	0.308 O.D. steel sleeve ↓
8718 ↓	PVA PVA PVA PVA/PETN <sup>d</sup> ↓ PVA/PETN <sup>d</sup> ↓	2.40 ± 0.05  3.05 ± 0.10/ 1.42 ± 0.02 3.05 ± 0.10/ 1.42 ± 0.02	Pyrex ↓	4 ↓	none ↓	C C M C  M	1.00 ↓	1.78 2.00 1.82 1.88  1.97	1.86 1.93	Black box ↓
8792 ↓	PVA PVA PVA/PETN <sup>d</sup> ↓	2.40 ± 0.05 2.40 ± 0.05 3.05 ± 0.10/ 1.42 ± 0.02	Pyrex ↓	8 ↓	none ↓	St St St	-- --	1.02 1.05 1.01	1.04	308" O.D. steel sleeve
8981 ↓	PVA ↓	2.40 ± 0.05 ↓	Pyrex ↓	8 ↓	none ↓	St M C St St St	1.00 ↓	0.81 0.94 0.85 0.85 0.84 0.90	0.87	
8982 ↓	PVA ↓	2.40 ± 0.05 ↓	Pyrex ↓	4 ↓	none ↓	S C C St S	0.94 ↓	0.76 0.70 0.77 0.69 0.83	0.76	
8983 ↓	PVA ↓	2.40 ± 0.05 ↓	Pyrex ↓	2 ↓	none ↓	C C M U St C	0.91 ↓	1.10 1.04 0.99 1.04 1.01 1.09	1.04	Black box ↓

Table VI continued

SHOT NO.	AZIDE	DENSITY (g/cc)	CONFINEMENT	MIRRORBOX LENGTH (inches)	FILTER	LIGHT BREAK-OUT†	RELATIVE INTENSITY I <sub>s</sub>	INITIATION DELAY (μsec)	AVG DELAY (μsec)	REMARKS
9022	PVA PVA PVA PVA/PEIN <sup>d</sup> PVA/PEIN <sup>d</sup> PVA/PEIN <sup>d</sup>	2.40 ± 0.05 2.40 ± 0.05 2.40 ± 0.05 3.03 ± 0.15/ 1.34 ± 0.06 3.03 ± 0.15/ 1.34 ± 0.06 3.03 ± 0.15/ 1.34 ± 0.06	Pyrex ↓	8 ↓	none ↓	-- -- -- St T C	-- -- -- -- -- --	0.99? 0.94? 0.96? 0.87 0.88 0.84	0.96? 0.86	
9044	PVA ↓	2.40 ± 0.05 ↓	Pyrex Pyrex Pyrex Crown Crown Crown Crown Crown	4 ↓	none ↓	St St St St M U S St	-- -- -- -- -- -- -- --	0.64 0.71 0.67 0.75 0.82 0.80 0.75 0.78	0.67 0.79 0.77	10-mil confinement 10-mil confinement
9042	PVA ↓	2.40 ± 0.05 ↓	Pyrex Crown Crown Crown	8 ↓	none ↓	S S C C	0.97 0.97 0.97 0.97	0.90 1.10 1.03 1.01	-- 1.05	
9043	PVA PVA PVA/PEIN <sup>d</sup> ↓ PVA PVA	2.40 ± 0.05 2.40 ± 0.05 3.05 ± 0.1/ 1.42 ± 0.02 2.40 ± 0.05 2.40 ± 0.05	Crown Crown Pyrex ↓ Crown Crown	8 ↓	none ↓	M C St  St St S St St St B	-- -- --  -- -- -- -- -- -- --	0.95 1.02 0.94  0.91 0.88 0.94 0.96 0.88 0.94 1.05 1.14	0.99 0.91   0.95 0.95 0.91 1.09	at 21.5° from vertical at 21.5° from vertical at 26.5° from vertical at 26.5° from vertical at 18.7° from vertical at 18.7° from vertical
9221	PVA PVA PVA Colloidal Colloidal Colloidal	2.30 ± 0.02 2.30 ± 0.02 2.30 ± 0.02 2.53 ± 0.02 2.53 ± 0.02 2.53 ± 0.02	Pyrex ↓	8 ↓	none ↓	S S S C S C	-- -- -- -- -- --	0.67 0.78 0.74 0.77 0.86 0.81	0.73 0.81	U.V. reflecting mirror ↓
9222	PVA PVA PVA PVA Colloidal Colloidal Colloidal	2.30 ± 0.05 2.30 ± 0.05 2.30 ± 0.05 2.30 ± 0.05 2.51 ± 0.03 2.51 ± 0.03 2.51 ± 0.03	Pyrex ↓	4 ↓	none ↓	U S S S U St C	-- -- -- -- -- -- --	0.61 0.61 0.58 0.65 0.63 0.71 0.65	0.61 0.66	U.V. reflecting mirror ↓
9252	PVA PVA Colloidal Colloidal Colloidal PVA (pale) PVA (pale) PVA (pale)	2.40 ± 0.05 2.40 ± 0.05 2.63 ± 0.02 2.63 ± 0.02 2.63 ± 0.02 2.40 ± 0.05 2.40 ± 0.05 2.40 ± 0.05	Pyrex Pyrex Pyrex Pyrex Pyrex Crown Crown Pyrex	4 ↓	none ↓	S C C St St U U U	-- -- -- -- -- -- -- --	0.76 0.71 0.78 0.86 0.85 1.11 1.19 0.89	0.74 0.83 1.15	U.V. reflecting mirror ↓

Table VI continued

SHOT NO.	AZIDE	DENSITY (g/cc)	CONFINEMENT	MIRRORBOX LENGTH (inches)	FILTER	LIGHT BREAK-OUT	RELATIVE INTENSITY %	INITIATION DELAY $\Delta$ ( $\mu$ sec)	AVG DELAY ( $\mu$ sec)	REMARKS
9253	PVA	2.40 $\pm$ 0.05	Pyrex	4	none	S	--	1.88	1.86	U.V. reflecting mirror 2 x 2" at Comp B encl. 4 x 4" at azide end
						B	--	1.92		
						C	--	1.84		
						S	--	1.84		
						C	--	1.83		
						C	--	1.76		
						B	--	1.89		
						M	--	1.92		
						B	--	1.70	1.74	
	PVA/Formvar 85/15 PVA/Formvar 85/15	2.25 $\pm$ 0.01 2.25 $\pm$ 0.01				St	--	1.77		
9253	PVA	2.26 $\pm$ 0.02	Crown Crown	4		S	--	2.08	2.24	
	PVA	2.26 $\pm$ 0.02				C	--	2.42		
8679	PVA	2.40 $\pm$ 0.05	Quartz	8	none	S St	0.93	0.64 0.62	0.63	
8680	PVA	2.40 $\pm$ 0.05	Quartz	8	none	S S	0.81	0.76 0.77	0.77	
8681	PVA	2.40 $\pm$ 0.05	Quartz	8	none	S C	~0.81	1.87 1.88	1.88	Black Box
9221	PVA	2.16 $\pm$ 0.01	Quartz	8	none	S S	--	0.45 0.48	0.465	U.V. reflecting mirror
9222	PVA	2.19 $\pm$ 0.02	Quartz	4	none	S S	--	0.36 0.39	0.38	U.V. reflecting mirror
8718	PVA	2.44 $\pm$ 0.01	7-54	4	none	T C	1.00	1.36 1.42	1.39	Black Box
8983	PVA	2.42 $\pm$ 0.05	7-54	2	none	ST U	0.91	0.76 1.01	--	Black Box Black Box, scratch on 7-54
8580	PVA	~2.2	Pyrex	8	0.3N.D	C	--	3.60		
8576	PVA	~2.2	Pyrex	8	0.3N.D	T	--	3.38		
8679	PVA	2.40 $\pm$ 0.05	Pyrex	8	0.3N.D	B S	0.93	2.31 2.99		
8680	PVA	2.40 $\pm$ 0.05	Pyrex	8	0.3N.D	C	0.81	2.80		
8720	PVA	2.40 $\pm$ 0.05	Pyrex	8	0.3N.D	S C	1.00	2.52 2.63		
9044	PVA	2.40 $\pm$ 0.05	Pyrex	4	0.3N.D	M	--	1.70		
8679	PVA	2.40 $\pm$ 0.05	Pyrex	8	0.2N.D	C S	0.93	1.80 2.01	1.90	
8718	PVA	2.40 $\pm$ 0.05	Pyrex	4	0.2N.D	T M	1.00	3.92 4.47	4.19	Black Box
8983	PVA	2.40 $\pm$ 0.05	Pyrex	2	0.2N.D	C B	0.91	1.95 1.64	1.80	Black Box
8982	PVA	2.40 $\pm$ 0.05	Pyrex	4	0.2N.D	M C	0.94	1.44 1.43	1.44	

Table VI concluded

SHOT NO.	AZIDE	DENSITY (g/cc)	CONFINEMENT*	MIRRORBOX LENGTH (inches)	FILTER	LIGHT BREAK-OUT†	RELATIVE INTENSITY I §	INITIATION DELAY Δ (μsec)	AVG DELAY (μsec)	REMARKS
8681	PVA	2.40 ± 0.05	Pyrex	8	0.1N.D.	M C	~0.81	10.03 10.10	10.07	Black Box
8718	PVA	2.40 ± 0.05	Pyrex	4	0.1N.D.	U	1.77	2.94	--	Black Box
8983	PVA	2.40 ± 0.05	Pyrex	2	0.1N.D.	S U	0.91	1.59 1.63	1.61	Black Box
8982	PVA	2.40 ± 0.05	Pyrex	4	0.1N.D.	C B	0.94	1.01 1.06	1.04	
9044	PVA	2.40 ± 0.05	Pyrex	4	0.1N.D.	St U	--	0.91 0.94	0.93	
9221	PVA	2.26 ± 0.02	Pyrex	8	0.1N.D.	S S	--	1.02 1.07	1.05	U.V. reflecting mirror
9222	PVA	2.31	Pyrex	4	0.1N.D.	C	--	0.85	--	U.V. reflecting mirror
8679	PVA	2.40 ± 0.05	Pyrex	8	1A	T C	0.93	3.03 3.07	3.05	
8680	PVA	2.40 ± 0.05	Pyrex	8	1A	St C	0.80	3.22 3.17	3.20	
8584	PVA	2.20 ± 0.05	Pyrex	8	0-52	C	0.68	1.79	--	
8680	PVA	2.40 ± 0.05	Pyrex	8	0-52	C	0.81	1.59		
8983	PVA	2.40 ± 0.05	Pyrex	2	0-52	M	0.91	1.49		Black Box
8982	PVA	2.40 ± 0.05	Pyrex	4	0-52	St C	0.94	1.19 1.31	1.25	
8680	PVA	2.40 ± 0.05	Pyrex	8	7-54	M	0.80	2.19	--	
8681	PVA	2.40 ± 0.05	Pyrex	8	7-54	T B	~0.81	10.00 12.63	--	Black Box

\* Azide pressed against confining material

† Observed light "signals" were as sketched

$$\begin{array}{c}
 C \\
 St \\
 S \\
 U \\
 T \\
 B \\
 M
 \end{array}
 \begin{array}{c}
 ) \\
 | \\
 < \\
 / \text{ or } \backslash \\
 / \\
 \backslash \\
 \sim
 \end{array}$$

$$\S \quad \frac{I_{\text{peak}} \int_0^T I_{\text{rel}} dt}{(I_{\text{peak}})_{\text{max}} \int_0^T (I_{\text{rel}})_{\text{max}} dt}$$

Δ Total observed delay minus transit time through pellet

a 1/3 mil aluminized Mylar in contact with Comp B

b 2-mil aluminized Mylar in contact with Comp B

c PETN is around 250 μ

d PETN is around 80 μ

# (7) NORMALIZATION OF INITIATION DELAYS

A quick perusal of Table VI reveals that the jitter of initiation delays in any given shot is usually small. Variation in initiation delays from shot to shot can, however, be quite large. To treat all the data, some normalization scheme is obviously required. If  $I_{max}$  is the average of the three highest observed relative intensities and  $I_n$  is the peak intensity in any other shot, then the adopted normalization factor  $\bar{N}$  (a theoretical justification will be presented later) is  $(I_n/I_{max}) \times (\bar{I}_n/\bar{I}_{max})$  where  $\bar{I}$  was defined in Eq. (6). Normalized delays ( $\tau_{obs} \times \bar{N}$ ) for various window-filter combinations are shown in Table VII. It is obvious that the window-filter combination strongly influences initiation delay. A discussion of this effect will take up most of the next section.

Table VII  
NORMALIZED INITIATION DELAYS OF PVA LEAD AZIDE

WINDOW*	FILTER	SHOTS	OBSERVATIONS	MIRROR BOX LENGTH (inches)	AVERAGE $\tau$ ( $\mu$ sec)	RANGE ( $\mu$ sec)	REMARKS
Pyrex	none	9	45	8	0.88	0.79-0.98	Max. and min. $\tau$ occurred in same shot
Crown	none	3	8	8	1.02	0.98-1.07	Max. and min. $\tau$ occurred in same shot
Crown (10 mil)	none	1	2	8	0.95	0.90-1.00	
Quartz	none	2	4	8	0.60	0.58-0.62	
Pyrex	0.3 N.D.	3	5	8	2.46	2.15-2.78	Max. and min. $\tau$ in same shot
Pyrex	0.2 N.D.	1	2		1.77	1.67-1.87	
Pyrex	0.2 N.D.	3	6	8	1.73	1.59-1.87	Includes 2 previous shots <sup>1</sup>
Pyrex	1A	3	5	8	2.74	2.54-2.92	
Pyrex	0-52	7	8	8	1.35	1.22-1.41	Includes 5 previous shots <sup>1</sup>
Pyrex	7-54	7	7	8	1.73	1.71-1.76	Includes 6 previous shots <sup>1</sup>
Pyrex	none	2	10	4	0.70	0.64-0.81	
Crown	none	1	3	4	0.79	0.75-0.82	
Pyrex	0.2 N.D.	1	2	4	1.35	1.34-1.36	
Pyrex	1.0 N.D.	2	4	4	0.95	0.91-0.98	
Pyrex	0-52	1	2	4	1.18	1.12-1.23	

\* In contact with the azide.

# (8) NATURE OF RADIATION OF SHOCKED ARGON

To understand the relationship between absorbed energy and initiation delay (window/filter effect of Tables VI and VII) requires the knowledge of the radiation distribution and temperature of shocked argon. Using the photomultiplier-interference filter system described in Secs. 2, b(9) and 2, b(10) and Eq. (2) it was found (Table VIII) that the directly viewed argon radiation (small scale shots) is blackbody or at least graybody. In the streak-camera shots the argon radiation was reflected from the upper surface of the streak camera slit holder to the photomultiplier. As shown in figure 12 the reflectivity of the slit holder varies with wavelength. If  $R_{\lambda}^0$ , to distinguish it from  $R_{\lambda}$ , (the azide reflectivity) is the diffuse reflectivity of the slit holder, then the integrands of Eq. (2) have to be changed to  $N_{\lambda} A_{\lambda} R_{\lambda}^0$ . With this change, calculations based on photomultiplier observations of streak-camera shots also show that the argon radiation is blackbody (Table VIII).

# (9) TEMPERATURE OF SHOCKED ARGON

As discussed in Sec. 2, b(10), Eq. (2) cannot give  $T_a$ , the temperature of shocked argon. To get  $T_o$  it is necessary to make comparisons

Table VIII  
BLACKBODY DISTRIBUTION OF A COMP B SHOCK IN ARGON

FILTERS	OBS. OUTPUT VOLTS	OUTPUT RATIO	$\epsilon \int_{\lambda_1}^{\lambda_2} N_{\lambda} A_{\lambda} R_{\lambda}^0 d\lambda$ RATIO*
600 + No. 8 + 2.35 N.D. <sup>a</sup>	0.168, 0.163	0.197	0.186
500 + 1 A + 2.35 N.D. <sup>a</sup>	0.81, 0.85	1.000	1.000
450 + 1 A + 2.35 N.D. <sup>a</sup>	0.81, 0.78	0.957	0.995
400 + 1 A + 2.35 N.D. <sup>a</sup>	0.40	0.481	0.510
0.1 N.D. <sup>b</sup>	13.8 (13.6-14.1) <sup>c</sup>	1.000	1.000
450 + 1 A <sup>b</sup>	6.65 (6.2-6.7) <sup>c</sup>	0.481	0.482
400 + 1 A <sup>b</sup>	3.8 (3.7-3.9) <sup>c</sup>	0.282	0.276

\* See equation 2 and Section 2, c(8).

For  $T_o = 28000^{\circ}\text{K}$ ; the integral ratio is very nearly independent of  $T_o$  for  $22000^{\circ}\text{K} > T_o < 40000^{\circ}\text{K}$ ,  $R_{\lambda}^0$ , the reflectivity of the slit holder, is included only in the streak camera shots.

<sup>a</sup> Small-Scale Shot

<sup>b</sup> Streak Camera Shots

<sup>c</sup> Ratios of shots to Xe "Flasher"

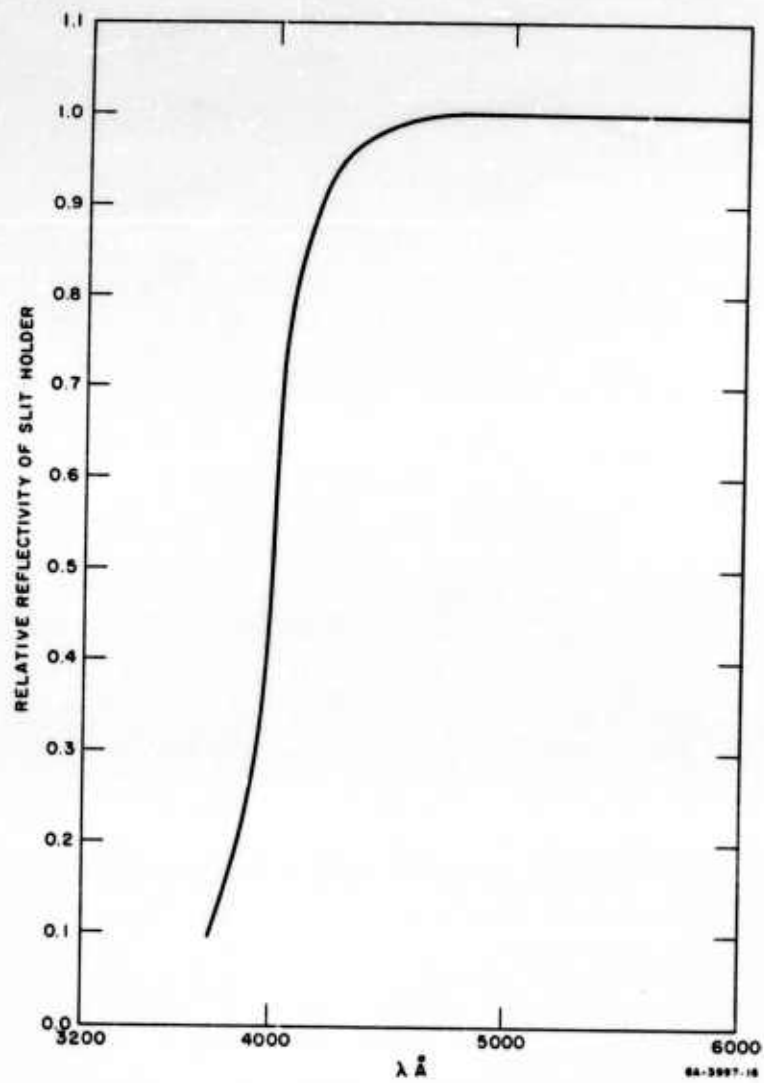


Figure 12 DIFFUSE REFLECTIVITY OF STREAK CAMERA SLIT HOLDER

with a standard temperature source. Because the photomultiplier output ratios are proportional to the radiance ratios, and these are

$$\frac{N_{\lambda}}{N'_{\lambda}} = \frac{e^{c_2/\lambda T'} - 1}{e^{c_2/\lambda T_a} - 1}$$

it is necessary to know  $T'$  very accurately if  $T_a \gg T'$  as it is in these measurements. Three different optical pyrometers, read by three different operators, gave an average  $T'$  of 2377°K and maximum spread of 2370-2380°K. In this temperature range Eq. (2) can be used, i.e., the integral ratio is quite sensitive to  $T'$ , and leads to  $T' = 2380^\circ\text{K}$ . The excellency of agreement between photomultiplier and pyrometer measurements is a strong argument for the essential correctness of the photomultiplier response curve obtained in this laboratory.

Using  $T' = 2380^\circ\text{K}$  and the measured output ratios in Eq. (3) gives the  $T_a$  values shown in Table IX. The temperature based on the 6000 Å interference filter is probably the least accurate because  $P_{\lambda}$ , the photomultiplier response, changes rapidly in this region and there could be some error in calculating it by Eq. (1). It seems likely that  $29,000 \pm 1000^\circ\text{K}$  is a reliable estimate of  $T_a$ . Model<sup>7</sup> gives  $T_a$  of 30,000°K and claims blackbody distribution, but does not specify the explosive used to generate the shock. He does give a fantastically high shock velocity of 18 mm/μsec. Comparison of  $T_a$  with the theoretical calculations of Bond<sup>2</sup> are made in Appendix B.

Some miscellaneous temperature measurements based on  $T_a = 29,000^\circ\text{K}$  are given in Table IX(a).

#### (10) DIAMETER EFFECT

Figure 13 shows that initiation delay is independent of azide column diameter until diameters become smaller than 0.10 inch. Thus azide diameter is unimportant for most of the measurement made in this study. It has been observed<sup>8</sup> that a lead-covered lead azide detonating fuse propagates stably at the very low velocity of 0.3 mm/μsec in diameters below 0.02 inch and for loading densities of around 4.3 g/cc. It is believed that at least a portion of the azide in diameters below 0.10 inch propagates at a low velocity (not necessarily the very low



Table IX  
MEASURED TEMPERATURE OF COMP B SHOCK IN ARGON  
(8.3 mm/ $\mu$ sec)

FILTERS	$T_a$ °K	$\frac{\epsilon_\lambda \int_{\lambda_1}^{\lambda_2} N_\lambda' A_\lambda P_\lambda d\lambda}{\epsilon_\lambda' \int_{\lambda_1}^{\lambda_2} N_\lambda' A_\lambda P_\lambda d\lambda}$ †	OBSERVED OUTPUT ARGON/STD
600 + No. 8 + 2.35 N.D.	31,500	286	288
500 + 1 A + 2.35 N.D.	30,000	922	926
450 + 1 A + 2.35 N.D.	29,000	1,910	1,940
400 + 1 A + 2.35 N.D.	29,000	2,860	2,870

\* To the nearest 500°K

† Primed quantities are for Standard Tungsten Ribbon;  $T' = 2380^\circ\text{K}$   
(see equation 3)

Table IX(a)  
MISCELLANEOUS TEMPERATURE MEASUREMENTS OF COMP B SHOCKS IN ARGON  
(all with B & L 450 interference filter)

GAS	COMP B COVER	ADDITIONAL FILTERS	OUTPUT RATIO	$\frac{\epsilon_\lambda \left[ \left( \frac{c_2}{\lambda T'} \right) - 1 \right]}{\epsilon_\lambda' \left[ \left( \frac{c_2}{\lambda T} \right) - 1 \right]}$	$(T_K)$
Argon	none	2.3 N.D. + 1 A	1.00	1.00	29,000
Argon	1-mil alum. Mylar	2.3 N.D. + 1 A	0.920	0.93	27,500
Argon	5-mil stainless st.	2.3 N.D. + 1 A	0.635	0.643	23,500
Krypton	none	2.3 N.D. + 1 A	1.54	1.54	38,000
Argon	none	2.3 N.D.	1.00	1.00	29,000
Argon	1-mil alum. Mylar	2.3 N.D.	~1.1	1.11	~30,500
Argon	3/4-mil alum.	2.3 N.D.	~1.0	1.00	~29,000

\* Primed quantities are bare Comp B in argon;  
see Table IV for sensitivities.

velocity observed in Ref. 8). Light output from 3.5 g/cc lead azide in 0.091-inch-I.D. is very faint and the luminosity is recorded as from burning rather than from detonation.<sup>1</sup> The lower density and much lower confinement of the azide pellets (on a weight basis the lead covered detonating fuse has 5 to 10 times the confinement of the nylon sleeve azide assemblies) would be expected to exhibit a diameter effect at larger diameters than found for detonating fuse.

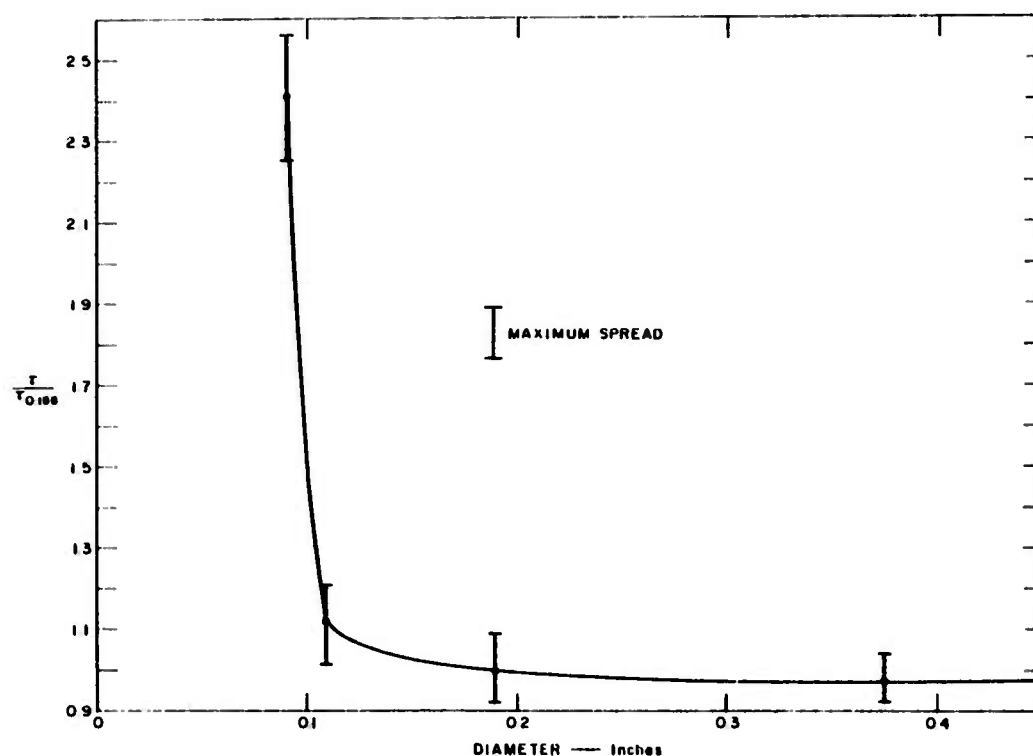


Figure 13 EFFECT OF AZIDE COLUMN DIAMETER ON INITIATION DELAY

### 3. DISCUSSION

#### a. FACTORS INFLUENCING INITIATION DELAY JITTER

##### (1) INCIDENT ENERGY

The energy flux as well as spectral region of the incident radiation is conveniently varied by placing filters between the argon shock and the azide window or by varying the window. As shown in Table VII the jitter about the average initiation delay stays roughly constant at about 10 percent for most of the window-filter combinations tried. Obviously this indicates the desirability of having short initiation delays to keep the absolute jitter small. The two materials which appear to have noticeably reduced jitter are quartz and Pyrex with a 7-54 filter. For the latter system no radiation above  $4000 \text{ \AA}$  gets to the azide and for the former most of the radiation reaching the azide ( $\sim 90\%$ ) is below  $4000 \text{ \AA}$ . Six other results (Table VI) indicate that jitter is indeed small for the quartz system. For the Pyrex and 7-54 system in black boxes jitter is large. It is also fairly large for 7-54 windows (no glass). Thus reduction of jitter by filtering out longer wavelength radiation is uncertain. Use of quartz windows, however, does appear to reduce both absolute and percent jitter. This was not the case in previous<sup>1</sup> work (using quartz of poorer optical quality) where jitters for the quartz and glass windows were quite comparable.

##### (2) FRONT-SURFACE CONFINEMENT AND PARTICLE SIZE

Figure 14 shows that raising a Pyrex window by as little as 1 mil above the azide surface facing the flash-bomb, greatly increases the initiation delay. Further raising of the window has relatively little effect. Thus, the region between 1-mil separation and intimate contact of azide and window is a region of great variation in initiation delay. It seems likely, therefore, that much of the jitter for the specimens with windows supposedly in contact with the azide could be caused by variations in the intimacy of contact. In the last shot of this investigation, it was noticed that in four assemblies some azide somehow got in between the top of the sleeve and the window (shot 9253, Table VI). For these four assemblies the average initiation delay was

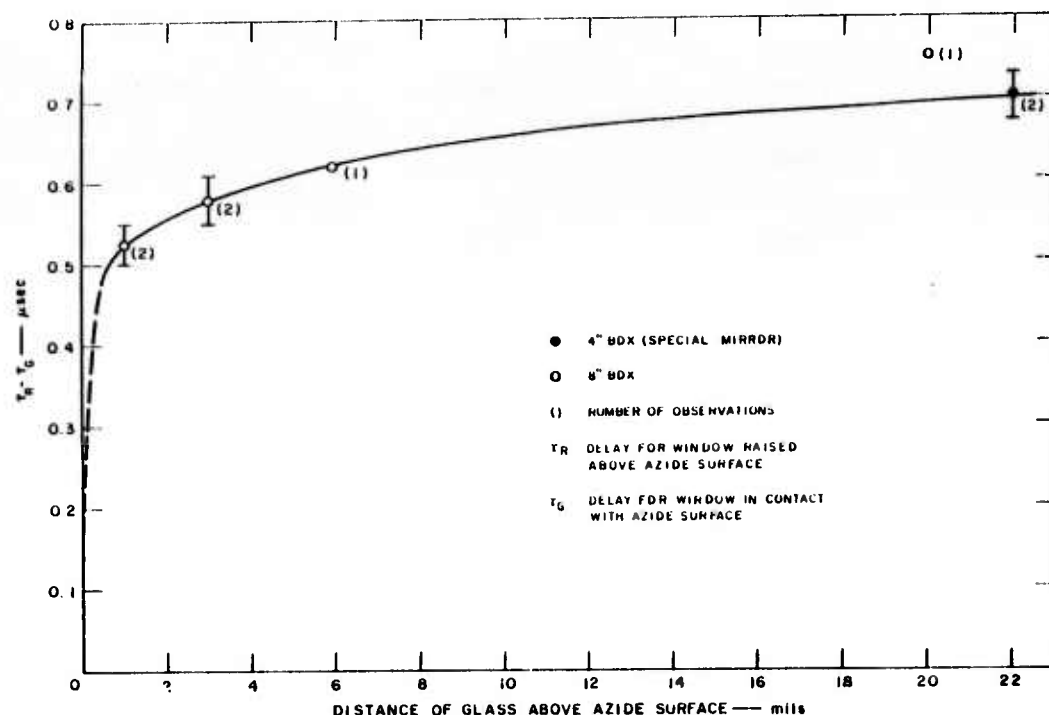


Figure 14 EFFECT OF INTIMACY OF FRONT-SURFACE CONFINEMENT ON INITIATION DELAY OF PVA LEAD AZIDE

1.90 (1.88 - 1.92)  $\mu\text{sec}$ . For four comparable normal assemblies in the same shot the average initiation delay was 1.82 (1.76 - 1.84)  $\mu\text{sec}$ .

Previous work<sup>1</sup> indicated that azide assemblies to which windows were attached after loading had, on an average, 0.15 to 0.20  $\mu\text{sec}$  longer initiation delays than normally loaded assemblies.

The greatly increased jitter found in the larger particle size azide (Fig. 15) is very likely caused by reduced intimacy of contact between azide and window.

### (3) EFFECT OF AZIDE PURITY AND PACKING DENSITY

Tables X and XI show that neither initiation delay nor delay jitter are affected by azide purity or packing density. The small increase in jitter at 3.3 g/cc is probably a manifestation of the diameter effect previously discussed. The small increase in initiation delay in

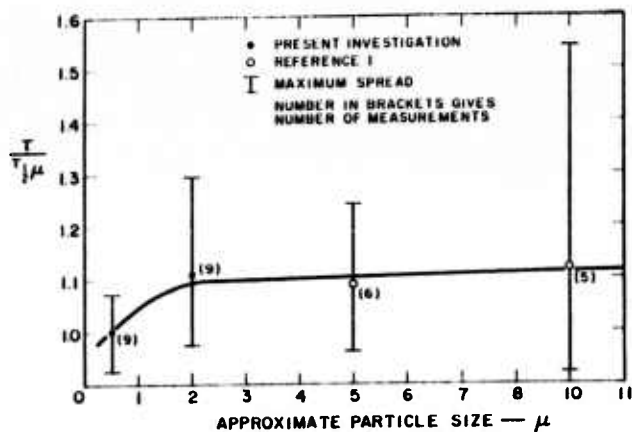


Figure 15 EFFECT OF AZIDE PARTICLE SIZE ON ITS INITIATION DELAY

Table X

EFFECT OF LEAD AZIDE PURITY ON INITIATION DELAY

AZIDE	OBSERVATIONS	RELATIVE INITIATION DELAY	RANGE
PVA	18	1.00	0.91-1.11
Colloidal <sup>a</sup>	9	1.11 <sup>b</sup>	1.03-1.15
90/10 PVA/Formvar	6	0.95	0.89-1.00
85/15 PVA/Formvar	5	0.99	0.91-1.06

<sup>a</sup> Very high purity

<sup>b</sup> See Fig. 15

Table XI

EFFECT OF PACKING DENSITY ON PVA LEAD AZIDE  
Initiation Delay

AZIDE DIAMETER (mils)	PACKING DENSITY (g/cc)	OBSERVATIONS	RELATIVE INITIATION DELAY	RANGE
188	2.2-2.4	10	1.00	0.96-1.08
188	2.5-2.6	9	1.11 <sup>a</sup>	1.03-1.18
188	3.0-3.2	9	1.03	0.97-1.08
375	1.6	8	0.97	0.92-1.04
109	3.3	5	1.12 <sup>b</sup>	1.01-1.21

<sup>a</sup> See Fig. 15

<sup>b</sup> See Fig. 13

colloidal azide, if real, might be caused by slightly different  $\alpha_\lambda$  and/or  $R_\lambda$  (not measured) from those found for PVA lead azide.

#### (4) INHERENT VARIABILITY OF AZIDE ASSEMBLIES

As shown in Table V there is appreciable variation in azide packing density and rather less variation in azide column height. Both these factors should influence transit times although no correlation between them and measured transit times has been found. Of course, any variation in transit time shows up as delay jitter. It is not known what portion of the appreciable variation in transit time is caused by measurement error and what portion is due to inherent variability of the separately loaded lead azide assemblies. The lack of correlation with packing density makes one suspect either random errors in packing-density measurements, or transit-time measurements, or both. Even if all the variability in the transit times of Table V were attributed to inherent variability of the azide assemblies, this would account for only about  $\frac{1}{3}$  of the observed initiation delay jitter.

#### (5) SUMMARY

It is believed that most of the observed jitter in the initiation delay of any given shot is caused by variations in the intimacy of contact between the azide and the window. A maximum of  $\frac{1}{3}$  of the observed jitter may be attributable to inherent variations in individually loaded lead azide assemblies.

#### b. DEPENDENCE OF INITIATION DELAY ON ENERGY ABSORPTION

##### (1) MODEL OF THE INITIATION PROCESS

For a better understanding of what is to follow, a qualitative picture of an argon flash-bomb initiation of lead azide will now be suggested. The quantitative consequences of this hypothetical model will be examined in the following sections:

- (a) Assume that the argon radiation absorbed by the azide appears primarily as heat and is used to raise the temperature of the azide.
- (b) Assume that there is no heat loss.

- (c) Assume that for most of the observed initiation delay there is no thermal decomposition of the azide and consequently no self-heating of the azide.
- (d) Assume that self-heating, i.e., thermal decomposition, after it starts, leads to thermal explosion and detonation in very short time.

A sketch of the expected temperature time profile in figure 16 may help clarify the above assumptions. Here  $\tau$  is the observed initiation delay,  $\tau_c$  is the time to reach  $T_c$  above which self-heating takes over,  $Q$  and  $c_p$  are heat of reaction and specific heat of lead azide,  $B$  is a constant characteristic of the system used, and  $f$  is the fraction of azide decomposed in time,  $\tau$ .

Since the argon radiation is blackbody [Sec. 2c(8)], as a consequence of assumptions (a), (b), and (c),  $dT/dt = \text{const.}$  for most of  $t$ . Because  $\tau$  is of the order of 1 to 6  $\mu\text{sec}$ , and  $T_c$  will be shown to be of the order of 900°K, assumption (b) appears to be sound, i.e., there is

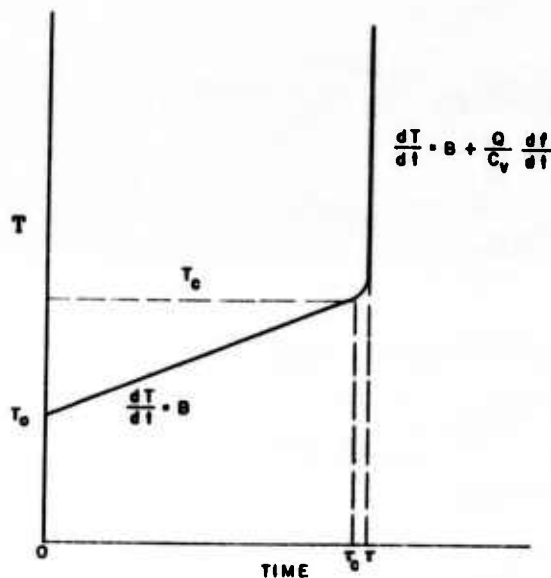


Figure 16 SKETCH OF THE POSTULATED TEMPERATURE-TIME PROFILE FOR THE INITIATION OF LEAD AZIDE BY RADIATION FROM A FLASH-BOMB

insufficient time for heat loss by conduction and  $T_c$  is too low for radiation to be important (Appendix C in Ref. 1). Since chemical reaction rate is controlled by the term  $\exp^{-E/RT}$ , where  $E$  is the activation energy of the rate controlling process and  $R$  is the gas constant, the abrupt change from no reaction to very rapid reaction seems reasonable, provided  $E$  is fairly large.

If the proposed model is correct, then initiation occurs very shortly after the azide temperature reaches  $T_c$ , regardless of the window-filter system used. Thus it is to be expected that

$$T_c' = \text{constant} = B\tau_c + T_0 \sim B\tau + T_0$$

since  $\tau_c$  was assumed to be very close to  $\tau$ . That  $B'\tau' + T_0' = B''\tau'' + T_0'' = \text{constant}$  can be tested experimentally by measuring initiation delays for different window-filter combinations placed between the azide and the flash bomb and also varying the ambient temperature. Before doing this a procedure for computing  $B$  must be established.

## (2) CALCULATION OF $B_0$

If  $I_0$  is the energy flux for a wavelength increment  $d\lambda$  incident on an azide increment of thickness  $dx$  and  $R$  is the reflectivity of the azide for the interval  $d\lambda$ , then the energy absorbed by  $dx$ , per unit time per unit area, is:

$$\bar{E}_{abs} = I_0(1 - R)\alpha\rho dx \quad (7)$$

where  $\alpha$  and  $\rho$  are the azide absorption coefficient and density. The heat capacity of the azide increment is  $\rho c_v dx$ . Consequently the temperature rise of the azide surface, assuming that the absorbed energy appears entirely as heat, is  $I_0(1 - R)\alpha/c_v$ . For a blackbody radiator, assuming no radiation loss due to geometric divergence of the radiation beam, the maximum rate of temperature rise of the irradiated azide surface is

$$B_0 = \frac{1}{c_v} \int_{\lambda_1}^{\lambda_2} A_\lambda(I_0)_\lambda(1 - R_\lambda)\alpha_\lambda d\lambda = \frac{1}{c_v} \int_{\lambda_1}^{\lambda_2} A_\lambda W_\lambda(1 - R_\lambda)\alpha_\lambda d\lambda \quad (8)$$



where  $A_\lambda$  is the transmission of the window-filter system at wavelength  $\lambda$ ,  $W_\lambda = \pi N_\lambda$  is the spectral radiance<sup>5</sup> of the argon at  $\lambda$  and  $T_0$ , and the limits of integration,  $\lambda_1$  and  $\lambda_2$ , are determined by the particular window-filter combination used.

Using blackbody tables,<sup>5</sup> a constant  $c_0$  given in Reference 16, and measured  $\alpha_\lambda$  and  $R_\lambda$ , Eq. (8) was evaluated numerically for  $T_0 = 29000^\circ\text{K}$  for various combinations of window-filters. The results are shown in column 5 of Table XIV. The numerical computation was also programmed to provide the fraction of  $B_0$  contained in selected wavelength intervals for various window-filter combinations. These are given in Table XII.

Table XII  
FRACTION OF ABSORBED ENERGY IN SELECTED  
WAVELENGTH REGIONS  
(4 Minute Suntan)

WINDOW	FILTER	WAVELENGTH REGION		
		Below 3300 Å	3300-4000 Å	4000-7000 Å
Pyrex	none	0.217	0.503	0.280
Pyrex	0.1 N.D.	0.165	0.507	0.328
Pyrex	0.2 N.D.	0.145	0.504	0.351
Pyrex	0.3 N.D.	0.134	0.497	0.369
Pyrex	0-52	0	0.497	0.503
Pyrex	7-54	0.326	0.662	0.012
Crown	none	0.086	0.576	0.338
Crown*	none	0.136	0.803	0.061
Quartz	none	0.782	0.143	0.075

\* "Pele"

### (3) CALCULATION OF RADIANT ENERGY LOSS

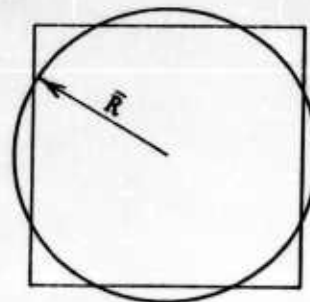
Unless the argon container walls are perfect reflectors at all wavelengths, not all the flash-bomb radiant energy will reach the window filter combination over the azide.\* The case for perfectly nonreflecting walls (black boxes) will be examined first. Since the flash bomb is a perfectly diffuse radiator (blackbody), standard geometric optics<sup>9</sup> gives

\* In Reference 1, it was incorrectly assumed that all the radiant energy of the flash bomb reaches the azide window-filter.

the fraction of energy,  $F$ , arriving from a flash bomb of equivalent radius,  $\bar{R}$ , at a surface of radius  $\bar{R}$  a distance  $L$  from the flash bomb:

$$F = \frac{\bar{R}^2}{\bar{R}^2 + L^2} \quad (9)$$

If  $\bar{R}$ , as shown in the sketch, is chosen to give the same area as the area of the square boxes used in this study, it can be shown that the error in using  $\bar{R}$  rather than the actual box cross-sectional dimension is very small. Using  $\bar{R}$  greatly simplifies the derivations about to be presented. Now Eq. (9) is for an energy source a fixed distance away. In actuality, the energy source advances toward the azide at a constant velocity,  $U$ , so that the distance between source and azide is continuously decreasing.



Accordingly an average  $F$  is

$$\frac{\int_0^\tau F dt}{\tau} = \frac{1}{\tau} \int_0^\tau \frac{\bar{R}^2 dt}{\bar{R}^2 + (L - Ut)^2}$$

which integrates to

$$\bar{F} = \frac{\bar{R}}{U\tau} \left[ \tan^{-1} \frac{L}{\bar{R}} - \tan^{-1} \left( \frac{L - U\tau}{\bar{R}} \right) \right] \quad (10)$$

Plots of  $\bar{F}$  vs.  $\tau$  are given in figure 17.

For square cross-section mirror walls, geometric optics gives the radii of equivalent circles required to have the light reach the azide surface in 1, 2, and  $n$  reflections, as  $3\bar{R}$ ,  $5\bar{R}$  and  $(1 + 2n)\bar{R}$ . The maximum  $\bar{F}$  obtainable for the  $n$ th reflection is given in figure 18 for  $L = 8$  inches or 4 inches. Of course the total fraction,  $\bar{F}_T$ , illuminating the azide directly and by reflection from the mirror walls is

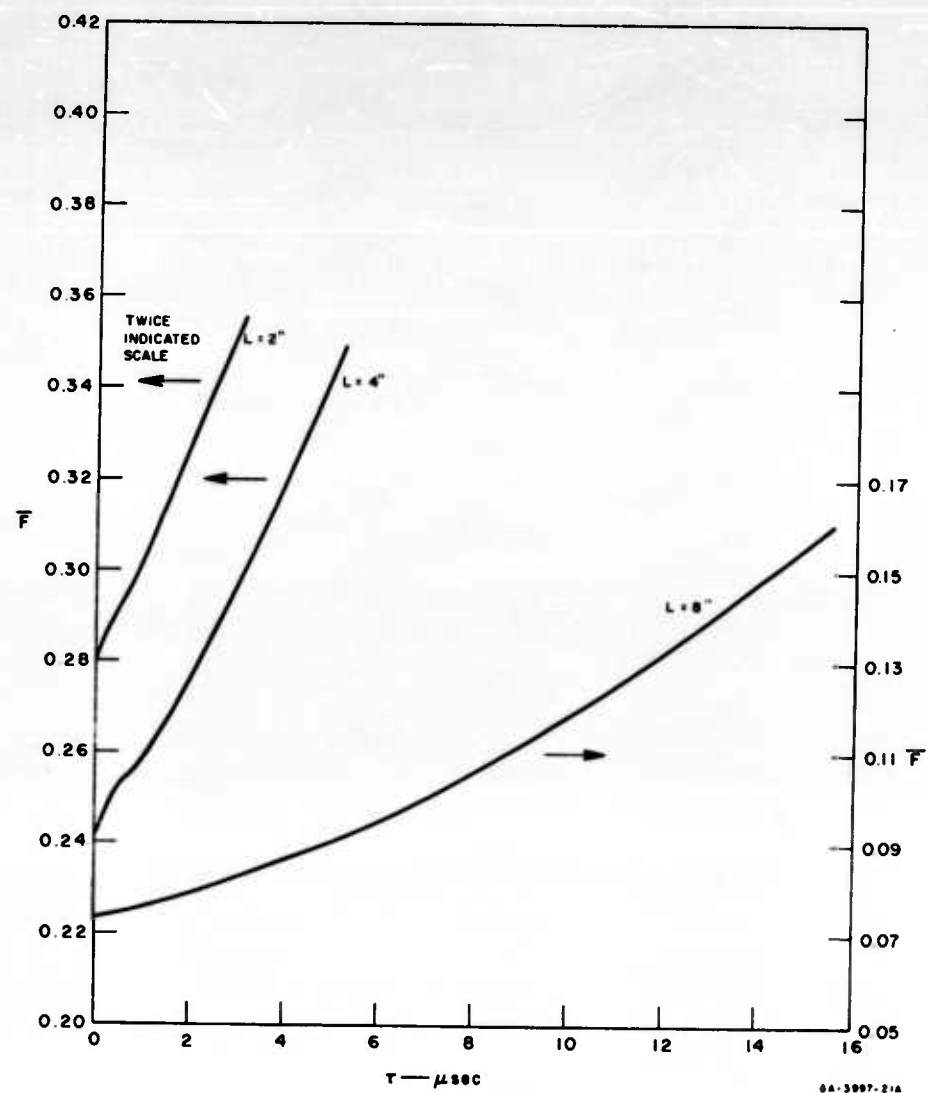


Figure 17 FRACTION OF RADIATED ENERGY REACHING 4-INCH  $\times$  4-INCH SURFACE FROM A RADIATOR STEADILY ADVANCING TOWARDS THE SURFACE (No reflections)

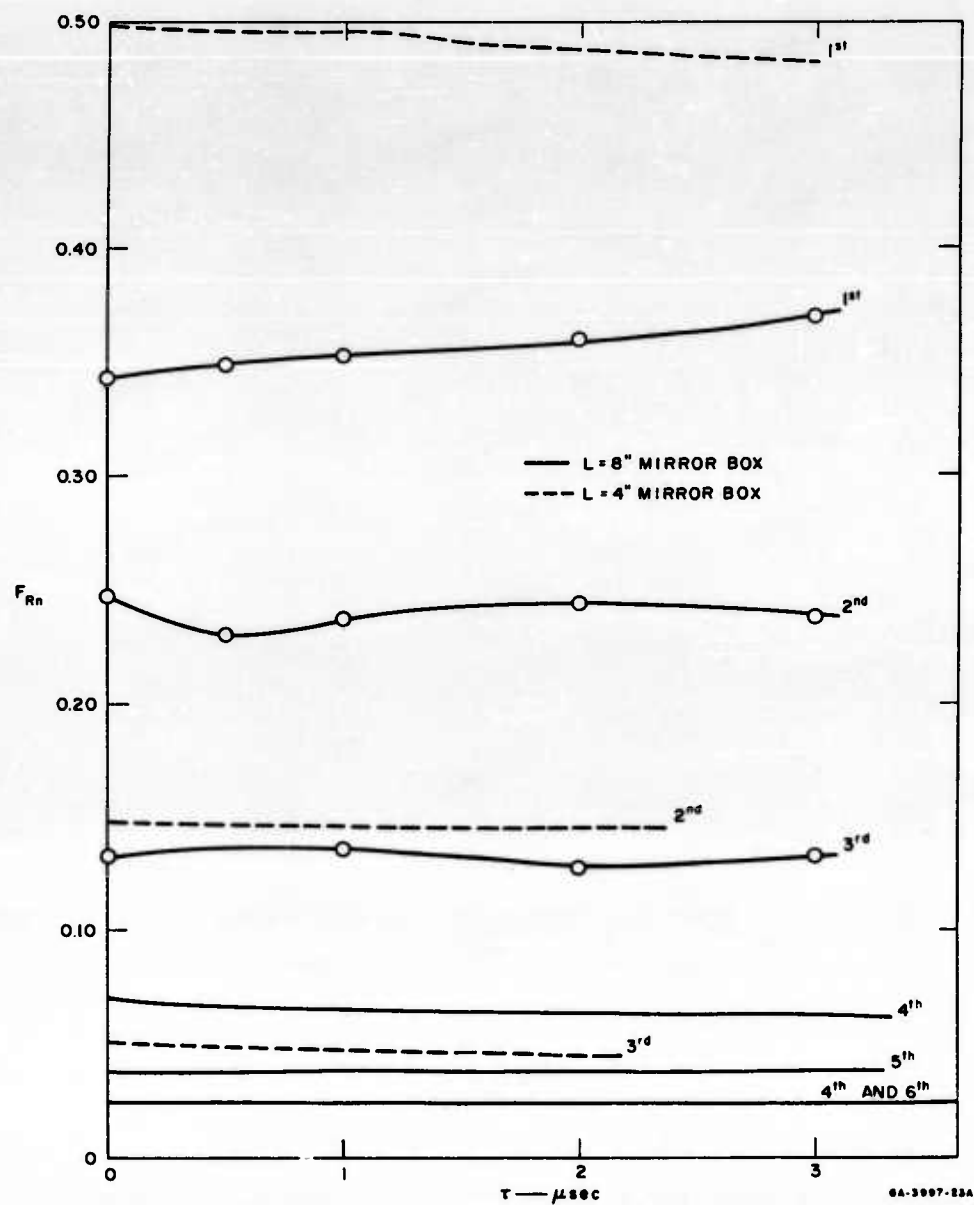


Figure 18 FRACTION OF ENERGY REACHING A 4-INCH  $\times$  4-INCH SURFACE FROM A RADIATOR STEADILY ADVANCING TOWARDS THE SURFACE (With reflections)

$$\bar{F}_T = \bar{F} + r_\lambda \bar{F}_{R_1} + r_\lambda^2 \bar{F}_{R_2} \dots, r_\lambda^n \bar{F}_{R_n} \quad (11)$$

As shown in figure 3, the mirror reflectivity,  $r_\lambda$ , changes with  $\lambda$ . Consequently it is necessary to define an average  $r_\lambda$  for selected wavelength intervals (the ones given in Table XII) as

$$\bar{r}_\lambda = \frac{\int_{\lambda_1}^{\lambda_2} N_\lambda r_\lambda d\lambda}{(\lambda_2 - \lambda_1) \int_{\lambda_1}^{\lambda_2} N_\lambda d\lambda} \quad (12)$$

where  $N_\lambda d\lambda$  is obtained from blackbody tables.<sup>5</sup> Average  $\bar{r}_\lambda$ 's are listed in Table XIII.

#### (4) CALCULATION OF $B$ FOR BLACK BOXES

As already discussed the relative light intensity of an argon flash bomb has a rise time which is of the same order as the shortest observed initiation delays. An effective relative light intensity was therefore defined and plotted as a function of  $\tau$  in figure 11. This effective intensity varies somewhat with  $\lambda$ . However the effective intensity obtained from photomultiplier records with neutral density filters appears to be a good average for the entire region (3000-6000 Å) to which most of the initiation experiments were restricted. If  $\bar{I}$  is the average effective intensity for white light (Fig. 11) then the rate of azide temperature rise  $B$ , is

$$B \sim B_0 \bar{F} \bar{I} \quad (13)$$

#### (5) CONSTANCY OF $B\tau$ FOR BLACK BOXES

A plot of measured  $\tau$  vs.  $1/B$ , as calculated from Eq. (13), is shown in figure 19. The straight line shown is for a least square fit forced through the origin. The slope is  $616 \pm 48^\circ\text{K}$  (the standard

Table XIII  
AVERAGE MIRROR REFLECTIVITIES\*  
FOR NORMAL INCIDENCE

WAVELENGTH INTERVAL	$\bar{r}_\lambda$	
	749	SPECIAL
Above 4000 Å	0.880	0.885
3300-4000 Å	0.865	0.875
3300-2900 Å	0.780	0.835
3300-2000 Å	~0.30	0.53

\* From measurement supplied by manufacturer, see Fig. 3

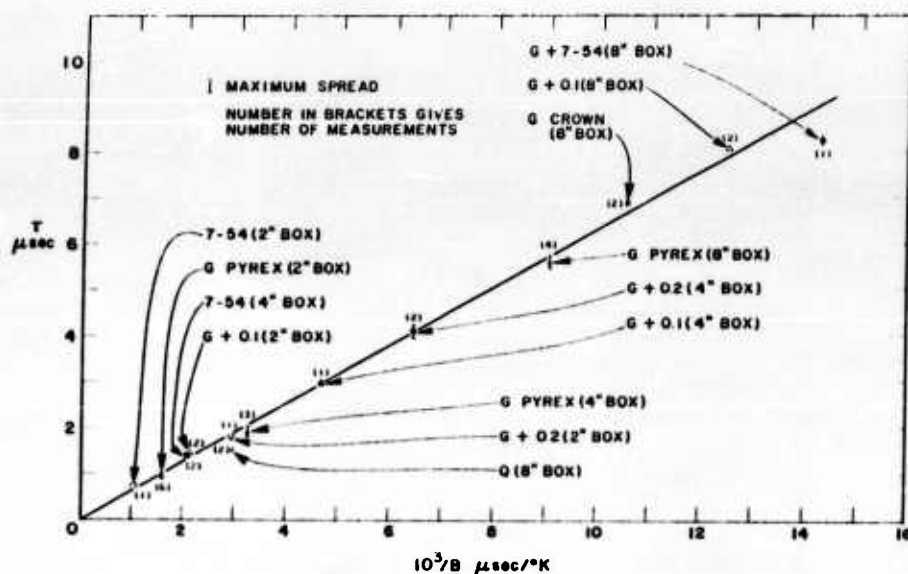


Figure 19 CONSTANCY OF  $B\tau$  FOR NONREFLECTING ARGON CONTAINERS

deviation). The constancy of  $B\tau$  provides a justification for the procedure adopted in normalizing initiation delays (Table VII).

#### (6) COMPUTATION OF $\tau_c$ FOR MIRROR BOXES

Because the computation of  $\bar{F}_T$  [Eq. (11)] for mirror boxes is cumbersome, and might contain sizeable uncertainties due to the approximate procedure for obtaining the average  $\bar{r}_\lambda$ 's, a different approach was used. If  $B\tau$  is constant for mirror boxes, as it appears to be for black boxes, then

$$\bar{F}_T = m/B_0 \bar{I}\tau \quad (14)$$

where  $m$  is the slope of figure 19 and  $\tau$  is the observed delay of a particular window-filter system (Table VI).  $\bar{F}_T$  for selected window-filter combinations and several types of mirror boxes was also calculated by Eq. (11). As shown in Table XIV agreement between the two methods is generally quite good. Because of large extrapolations in obtaining the  $\bar{r}_\lambda$  to be used in the quartz window system and some uncertainty in its  $B_0$ , close agreement between the two  $\bar{F}_T$ 's is not to be expected. The discrepancy for the Pyrex window with 7-54 filter remains unexplained.  $B\tau$ 's based on the mean values of the two  $\bar{F}_T$ 's are satisfactorily constant.

Table XIV  
"CRITICAL" TEMPERATURE RISE FOR PVA LEAD AZIDE

WINDOW	FILTER	$\tau$ ( $\mu\text{sec}$ )	$\frac{1}{I}$	$B_0$ ( $^{\circ}\text{K}/\mu\text{sec}$ )	LIGHT PATH INCHES	MIRROR REFLECTION		$\Delta T^{\S}$ ( $^{\circ}\text{K}$ )
						Apparent (%)	Calc. $\dagger$ (%)	
Pyrex	none	0.88	0.815	1,300	3	66.5	70	635
Crown	none	1.02	0.84	1,051		68.5	--	--
Crown <sup>o</sup>	none	1.25	0.86	783		73	72	610
Quartz	none	0.60	0.75	$\sim 5,000$		$\sim 24$	$\sim 32^b$	$\sim 630$
Pyrex	0.2 N.D.	1.73	0.895	555		71	73	620
Pyrex	0.3 N.D.	2.46	0.905	434		64	--	--
Pyrex	1 A	2.74	0.905	310		80	76	600
Pyrex	0-52	1.35	0.865	658		80	75	595
Pyrex	7-54	1.73	0.895	728		54.5	68	--
Pyrex <sup>c</sup>	none	0.73	0.79	1,300		82.5	74	585
Quartz <sup>c</sup>	none	0.48	0.69	$\sim 5,000$		$\sim 35$	$\sim 44^d$	$\sim 645$
Pyrex <sup>c</sup>	0.1 N.D.	1.04	0.85	835		83.5	--	--
Pyrex	none	0.70	0.765	1,300	4	88.5	84	600
Crown	none	0.79	0.795	1,052		93	--	--
Crown <sup>e</sup>	none	0.76	0.78	1,142		91	--	--
Pyrex	0.1 N.D.	0.95	0.82	835		95	--	--
Pyrex	0.2 N.D.	1.35	0.865	555		95	--	--
Pyrex	0.3 N.D.	1.70	0.890	434		94	--	--
Pyrex	0-52	1.18	0.85	658		93	87	595
Pyrex <sup>c</sup>	none	0.61	0.75	1,300		$\sim 100$	87	$\sim 555$
Quartz	none	0.38	0.62	$\sim 5,000$		49	$\sim 63^d$	$\sim 660$

\* From equation 14 and figure 19

$\dagger$  Calculated by equation 11 from reflectivity coefficients supplied by mirror manufacturer; normal incidence

$\S$  Based on average of "apparent" and "calculated"  $\bar{F}_T$

<sup>o</sup> "Pele" oxide; all other "sustained" 4 minutes

<sup>b</sup> Involves long extrapolation of reflectivity data.

<sup>c</sup> Special u.v. reflecting mirror

<sup>d</sup> Involves medium extrapolation of reflectivity data

<sup>e</sup> 10-mil-thick; all other glass 40-mil-thick

The average  $B\tau = T_c - T_0$  for all systems (including black boxes) is  $615 \pm 40^{\circ}\text{K}$  (standard deviation).

#### (7) INDEPENDENT DETERMINATION OF $B_0$

As already mentioned, a direct consequence of the proposed model is that

$$B\tau' + T'_0 \sim B\tau'' + T''_0$$

or

$$B_0 \bar{I}' \bar{F}'_{\tau'} + T'_0 = B_0 \bar{I}'' \bar{F}''_{\tau''} + T''_0 \quad (15)$$

In principle, a direct estimate of  $B_0$  is therefore possible from measurements of initiation delays  $\tau'$  and  $\tau''$  of identical azide assemblies contained in the same shot, but heated to different initial temperatures  $T'_0$  and  $T''_0$ .<sup>\*</sup> In practice, this experiment turned out to be rather complicated. To minimize measurement errors of initiation delay the difference in  $T'_0$  and  $T''_0$  should be made large (of the order of 200°C). At 200°C suntan fades rapidly (Ref. 1) which of course changes  $\alpha_\lambda$  and  $R_\lambda$ , and consequently  $B_0$ . To avoid this, untanned PVA lead azide was used. To ensure that it stayed "pale," the shot was fired at night. Unfortunately the shot was fired before it was realized that the crown glass windows used have appreciably less transmission below 4000 Å at 200°C than at room temperature and consequently  $B_0$  is not the same for  $T'_0$  and  $T''_0$ .

The measured transmissivity curves are shown in figure 20. The transmissivity curve for 220°C was obtained by interpolation.<sup>10</sup>

In the wavelength region where transmissivity is temperature dependent,  $\alpha_\lambda$  and  $R_\lambda$  are approximately constant (see Figs. 9 and 10). Therefore  $(1 - R_\lambda)\alpha_\lambda$  can be taken outside the integral and it follows that rewriting Eq. (8) gives

$$B_0 \simeq \frac{(1 - R_\lambda)\alpha_\lambda}{c_v} \int_{\lambda_1}^{4000} A_\lambda W_\lambda d\lambda + B_0 \phi = \frac{(1 - R_\lambda)\alpha_\lambda}{(1 - \phi)c_v} \int_{\lambda_1}^{4000} A_\lambda W_\lambda d\lambda$$

where  $\phi$  is the fraction of  $B_0$  contained in the wavelength region above 4000 Å (Table VI). For  $T_0$  equal to room temperature  $\phi$  is small and  $\phi'$  the fraction of  $B'$  at elevated starting temperatures although larger than  $\phi$  is also expected to be small. Consequently

$$1 - \phi \simeq 1 - \phi'$$

<sup>\*</sup> The experimental details of pre-heating the azide assemblies are described in Ref. 1.



$$\frac{B'_0}{B_0} = C \sim \frac{\int_{\lambda_1}^{4000} A'_\lambda W_\lambda d\lambda}{\int_{\lambda_1}^{4000} A_\lambda W_\lambda d\lambda} \quad (16)$$

By eliminating  $B'_0$  according to Eq. (16) and evaluating  $C$  numerically, Eq. (15) gives the following solution for  $B_0$

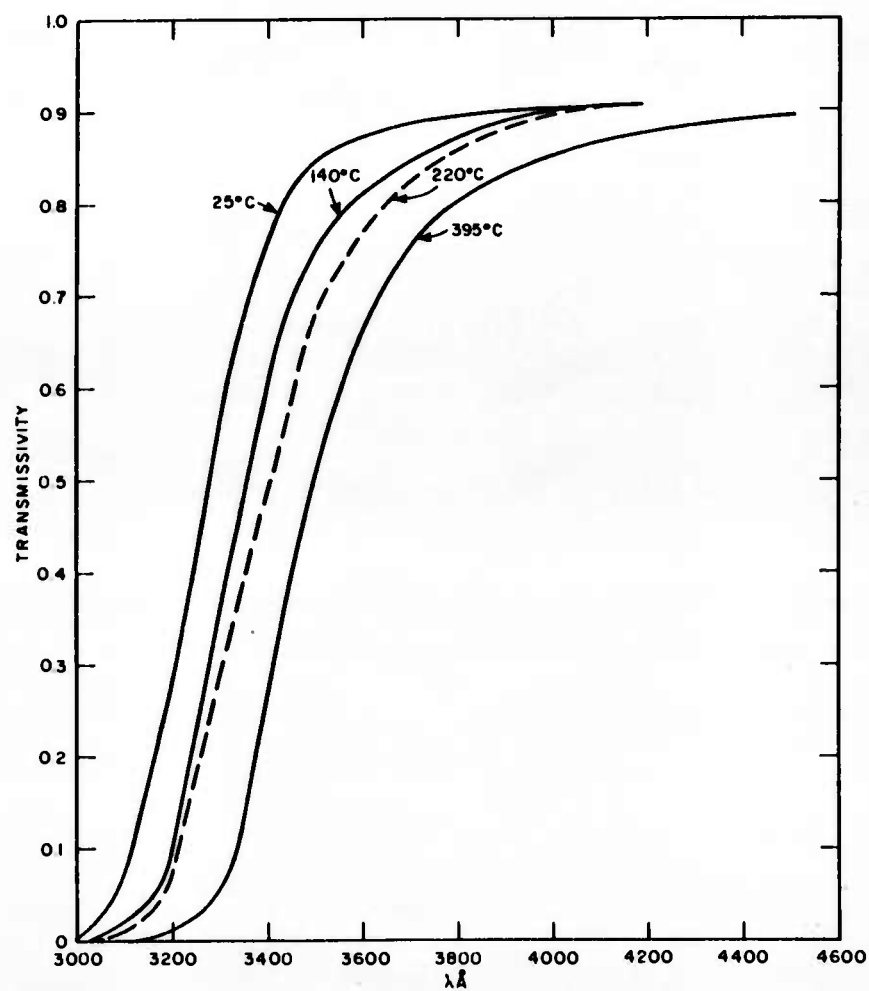


Figure 20 SPECTRAL TRANSMISSIVITY OF HEATED CROWN GLASS

$$B_0 \approx \frac{T_0'' - T_0'}{\bar{F}_T (\bar{I}' \tau' - C \bar{I}'' \tau'')} \quad (17)$$

An average  $\bar{F}_T$  is used since, as will be shown,  $\tau'$  and  $\tau''$  are not very different and according to figures 17 and 18 there is very little variation of  $\bar{F}$  or  $\bar{F}_T$  over short time intervals. Solutions of Eq. (17) using measured  $\tau$ 's are given below

$T_0$ (°C)	AVG $\tau$ ( $\mu$ sec)	RANGE ( $\mu$ sec)	$\bar{I}$	C	$\bar{F}_T B_0$ (°K/ $\mu$ sec)
10	1.42	1.35 - 1.51	0.88	1.00	--
140	1.29	1.27 - 1.33	0.87	0.86	456
220	1.13	1.11 - 1.17	0.855	0.78	424
				Avg	435

The normalization factor,  $\bar{N}$ , for this shot is 0.86 and  $\bar{F}_T$  is 0.725 (Table XIV, 3rd row) therefore  $\bar{F}_T B_0 / \bar{N} \bar{F}_T = B_0 = 700^\circ\text{K}/\mu\text{sec}$ , which agrees well with  $783^\circ\text{K}/\mu\text{sec}$  obtained from Eq. (8) with measured values of  $T_s$ ,  $A_\lambda$ ,  $\alpha_\lambda$  and  $\bar{R}_\lambda$ . Because of the approximations used in obtaining Eq. (16),  $B_0$  calculated by Eq. (17) is a close lower limit.

#### (8) ACTIVATION ENERGY OF LEAD AZIDE DECOMPOSITION

The preceding sections have shown that all the experimental results for azide assemblies with windows in contact with the azide lead to  $B\tau = \text{constant}$ . It now remains to be proved that  $\tau_e$  is indeed very close to  $\tau$  (Fig. 16) and that self-heating causes thermal explosion in a very short time. The heat balance equation, including self-heating, may be written in the form

$$\frac{dT}{dt} = B + \frac{Qdf}{c_v dt}$$

If the rate controlling process for the thermal decomposition is first order, this becomes

$$\frac{dT}{dt} = B + \frac{Q}{c_v} k(1-f) = B + \frac{Q}{c_v} Z e^{-E/RT} (1-f) \quad (18)$$

where  $Z$  is the frequency factor,  $E$  is the activation energy and  $f$  is the fraction of azide decomposed in time  $t$ .

Equation (18) was programmed for a Burroughs 220 computer and solved for  $T$  and  $f$  as functions of  $t$  for several values of  $E$ ,  $Z$ , and  $T_0$ .  $B$  was based on mean values of  $\bar{F}_T$  given in Table XIV and  $Q/c_p$ , according to the best literature values,<sup>16</sup> was taken as 3250°K. Some comments are in order about the choice of  $Z$  and  $T_0$ . In Table XIV it was shown that  $T_c - T_0 \sim 615^\circ\text{K}$ . Estimates of the melting point of lead azide range from 600 to 800°K.<sup>1,11</sup> It might therefore be expected that the lead azide melts before self-heating becomes appreciable. Since lead azide is a relatively simple molecule, and if it is indeed liquid, one might expect normal frequency factors of  $10^{13}$  to  $10^{14} \text{ sec}^{-1}$ . This simplifies the choice of  $Z$  but complicates the choice of initial temperature which now becomes  $T_0 - Q_f/C_p$ , where  $Q_f$  is the heat of fusion per gram of azide.

One might guess that  $Q_f$  is less than that for lead bromide which is 12 cal/g.<sup>15</sup> Accordingly  $T_0$  was taken as 300°K ( $Q_f = 0$ ) and 200°K ( $Q_f = 12 \text{ cal/g}$ ). Incidentally, the suppositions of the azide melting before much decomposition occurs would furnish a good explanation for the observed nondependence of  $\tau$  on particle size (Fig. 15).

The solution of Eq. (18) for Pyrex windows is shown in figure 21. The plots of both  $T$  and  $f$  are certainly of the expected form. Short interpolations were generally required to get the steep temperature rise to occur just prior to the observed  $\tau$ . Results are summarized in Table XV. Literature values of the activation energy for the thermal decomposition of lead azide obtained in the temperature interval of about 220 to 320°C range from 36 to 41 Kcal/mole.<sup>12,13,14</sup> Thus the approximately 36 Kcal/mole obtained for  $Z = 10^{14} \text{ sec}^{-1}$  and  $T_0 = 300^\circ\text{K}$  is in good agreement with the lower literature values. To get agreement for  $T_0 = 200^\circ\text{K}$ ,  $Z$  would have to be about  $10^{15} \text{ sec}^{-1}$ . For fixed values  $Z$  and  $T_0$ ,  $E$  varies directly with  $B$  for small changes in  $B$ .

#### (9) POSSIBILITY OF PHOTOCHEMICAL INITIATION

It has been proposed<sup>16</sup> that azides can be initiated by a truly photochemical process, which is rate controlling, followed by thermal explosion, namely,

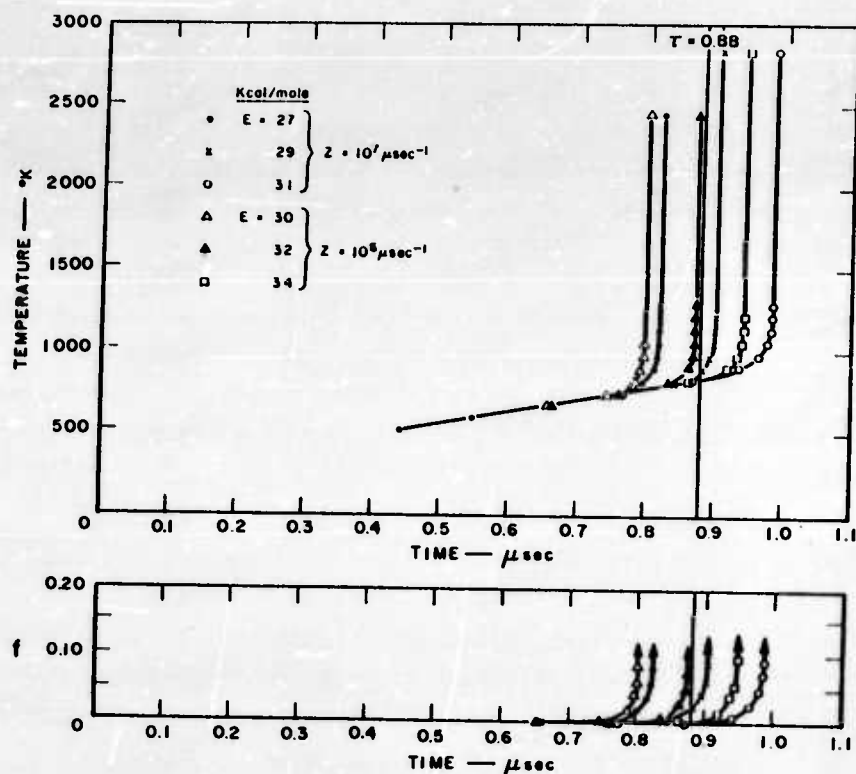
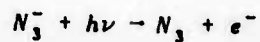


Figure 21 SOLUTIONS OF THE HEAT BALANCE EQUATION (Eq. 18)  
FOR PVA LEAD AZIDE WITH A PYREX GLASS WINDOW



$$N_3 \rightarrow \frac{3}{2} N_2 + 0.39 \text{ kcal/g azide decomposed}$$

It is believed that such a reaction can not be important in the present investigation for the following reasons:

From the definition of quantum yield<sup>17</sup>

$$f = \frac{\gamma M n}{\rho N dx}$$

Table XV  
ACTIVATION ENERGY FOR INITIATION OF PVA LEAD AZIDE

WINDOW	MIRROR BOXLENGTH (inches)	FILTER	$\tau$ ( $\mu\text{sec}$ )	$B^*$ ( $^\circ\text{K}/\mu\text{sec}$ )	$Z$ ( $\text{sec}^{-1}$ )	$T_0$ ( $^\circ\text{K}$ )	$E^\dagger$ (Kcal/mole)
Pyrex ↓	8	none	0.88	720	$10^{15}$	300	41.5
	↓	↓	↓	↓	$10^{14}$	300	36
	↓	↓	↓	↓	$10^{13}$	300	32
	↓	↓	↓	↓	$10^{15}$	200	36
	↓	↓	↓	↓	$10^{14}$	200	32.5
	↓	↓	↓	↓	$10^{13}$	200	28.5
	4	↓	0.70	855	$10^{14}$	300	36
	4	↓	0.70	855	$10^{13}$	300	31.5
	4	0.1 N.D.	0.95	620	$10^{14}$	300	36
	4	0.1 N.D.	0.95	620	$10^{13}$	300	32
	8	0.52	1.35	442	$10^{14}$	300	36.5
	8	0.52	1.35	442	$10^{13}$	300	32
	8	0.52	1.35	442	$10^{14}$	200	32
	8	0.52	1.35	442	$10^{13}$	200	28.5
	8	0.2 N.D.	1.73	358	$10^{14}$	300	38
	8	0.2 N.D.	1.73	358	$10^{13}$	300	33.5
	8	0.2 N.D.	1.73	358	$10^{14}$	200	34
	8	0.2 N.D.	1.73	358	$10^{13}$	200	30
	8	1A	2.74	219	$10^{14}$	300	37.5
	8	1A	2.74	219	$10^{13}$	300	33.5
	8	1A	2.74	219	$10^{14}$	200	34
	8	1A	2.74	219	$10^{13}$	200	30.5
Quartz	8	none	0.60	$\sim 1050^a$	$10^{14}$	300	36
Quartz	8	none	0.60	$\sim 1050^a$	$10^{13}$	300	32
Quartz	8	none	0.60	1315 <sup>a</sup>	$10^{14}$	300	42
Quartz	8	none	0.60	1315 <sup>a</sup>	$10^{13}$	300	37

\*  $B = B_0 \bar{I} \bar{F}_T$

† From numerical solutions of equation 18

<sup>a</sup> Depending on what  $\lambda$  is taken to be for u.v. see figura 3

where

- $n$  = number of quanta absorbed per unit area per unit time
- $f$  = fraction of azide decomposed
- $\gamma$  = quantum yield
- $N$  = Avogadro's number
- $M$  = azide molecular weight
- $\rho$  = azide packing density
- $dx$  = thickness of azide increment

At the irradiated surface, from  $E = h\nu$  and Eq. (8) the number of quanta absorbed per unit area per unit time at  $\lambda$  is

$$n_{\lambda} = \frac{W_{\lambda} A_{\lambda} (1 - R_{\lambda}) \alpha_{\lambda} \rho dx}{hc/\lambda}$$

and the total number of quanta absorbed in time  $\tau$  in interval  $\lambda_2$  to  $\lambda_1$  is

$$\tau \int_{\lambda_1}^{\lambda_2} n d\lambda \sim \frac{\tau \rho dx}{hc} \int_{\lambda_1}^{\lambda_2} \lambda W_{\lambda} A_{\lambda} (1 - R_{\lambda}) \alpha_{\lambda} d\lambda$$

which gives

$$f \sim \frac{\gamma M \tau}{N h c} \int_{\lambda_1}^{4000} \lambda W_{\lambda} A_{\lambda} (1 - R_{\lambda}) \alpha_{\lambda} d\lambda \quad (19)$$

The integral was evaluated numerically for the Pyrex window assembly. Its upper limit represents the absorption edge of single crystals of lead azide. Using  $\gamma = 0.07$  as given by Dodd<sup>20</sup> for 2537 Å,  $\tau = 0.88 \mu\text{sec}$ , and  $\bar{F}_{\tau} \bar{I} = 0.56$  (see Table XIV) gives an estimate of  $f \sim 0.011$  and

$$\Delta T = \frac{fQ}{c_v} \sim 35^{\circ}\text{C} \quad (20)$$

which is much too small to lead to thermal explosion. Possibly, arguments could be advanced that most of the reaction somehow occurs in very localized regions which consequently get much hotter than the neighboring regions. Generally such "hot-spot" reactions are characterized by great variability; which is not in line with the excellent reproducibility of the initiation delays observed in this study.

c. MISCELLANEOUS OBSERVATIONS WHICH ARE CONSISTENT WITH THE PROPOSED MECHANISM

Initiation delays are independent of azide column length. This agrees with the supposition that initiation starts very close to the azide surface facing the flash-bomb. The lack of a particle size effect, as already mentioned, is to be expected if the azide melts before much decomposition has occurred. For the same reason and also because the density terms cancel out in computing  $B_0$  [Eq. (8)] the nondependence of  $\tau$  on packing density is consistent with the proposed initiation model. The increased initiation delay, as already discussed, for small diameter assemblies is probably caused by slow detonation velocity of the lead azide. The previously observed<sup>1</sup> nondependence of  $\tau$  on degree of suntan (1 to 4 minute exposure) is understandable in terms of Eq. (8) because of the "compensation" of  $\alpha_\lambda$  shown in figure 10 (for a lesser suntan there is more absorption in the u.v. and less in the visible, and conversely for larger suntans). The strong effect of front surface confinement, also referred to as window effect, as well as the nature of the light breakout signal are puzzling. Some speculation as to their causes will be presented in the next section.

d. LIGHT SIGNALS FROM DETONATING LEAD AZIDE

Streak camera records (Fig. 5) of lead azide assemblies, initiated by the radiation from an argon flash, show that the break-out of light from the azide is quite variable. Some trends in light break-out were listed in Table II. If initiation starts uniformly all over the azide surface facing the flash-bomb, signals of the type "St." or "C" (Table II) would be expected. The majority of observed signals with colloidal lead azide, lead azide/Formvar mixtures, Pyrex and O-52, and lead azide/PETN composites are of this type. Rather unexpectedly, in the shorter mirror boxes breakout is usually "C" or "St." In these instances, the azide receives a high proportion of direct and singly reflected radiation. For

quartz windows the majority of signals is asymmetric which means<sup>1</sup> that initiation occurs all around the outer periphery of the azide column. For pale azide the signals vary, but are largely of the type "B" "T" or "U". No clear trends are apparent for most of the Pyrex or crown glass window assemblies. This is also true for windows which have been raised above the azide surface. Thus there appears to be no correlation between type of signal and degree of front-surface confinement.

In a very rough sort of way, for a given window-filter combination, the "St." or "C" signals are generally associated with the shorter initiation delays. It seems possible that signals observed with composites result from rapid establishment of the expected spherical detonation wave in the PETN, regardless of the type of signal coming from the azide. The azide in the composites was at a higher density than in other assemblies; therefore, it is also conceivable that their signals were originally of the "St." or "C" type. It has been observed that as little as  $\frac{1}{16}$  inch of lucite invariably changes any azide signal to the "C" type.

In shot 8982, there was a 0.025-inch air-gap between the rear faces of two azide assemblies and the usual lucite plate covering the back of the azide holder (Fig. 4). Both these assemblies gave "M" type light breakout. Most of the other assemblies in this shot which supposedly had no air gaps, produced "C" type breakouts. This may indicate that light breakout depends more on closeness of contact between azide and lucite plate than on the factors discussed above.

#### e. EFFECT OF FRONT-SURFACE CONFINEMENT

It has been shown that intimacy of contact between azide and windows can cause large variations in initiation delay. The causes behind this effect are not all clear. If no windows are used, initiation delays are longer and much more variable than with glass windows, even though the azide gets the full radiation of the flash-bomb.<sup>1</sup> Very often the light signals appearing at the rear surfaces are so faint as to be barely discernible. This suggests a low azide detonation velocity. However, strong signals are usually observed with windows raised above the azide surfaces. Thus, an explanation of these effects based on the lack of front-surface confinement somehow causing a low azide detonation velocity [Sec. 2, b(10)] seems unlikely. Sublimation or vaporization of unconfined, hot azide layers might offer an explanation, since such a process would abstract



energy, and also mechanically remove heated material from the main body of the azide. If the temperature is too low for appreciable vaporization it is also conceivable that liquid azide droplets (the temperature just prior to initiation appears to be high enough for fusion) in which thermal decomposition has just started are propelled outwards by the gases generated by the thermal decomposition. Of necessity, the above is pure speculation and critical experiments are needed to interpret the role of front-surface confinement.

#### 4. SURFACE INITIATION SYSTEMS

##### a. PLANE WAVE DEMONSTRATION

The applicability of a closely spaced array of individual lead azide assemblies, initiated by an argon flash-bomb, to the simplest surface initiation system—a plane wave—has been demonstrated in shots 8792 and 9022. In both shots lead azide/PETN composite assemblies were used to initiate  $\frac{1}{4}$ -inch-thick Comp B. The light of the Comp B detonation was viewed by the streak camera using 21 vertical slits. Schematic diagrams of the assembly of shot 9022 are shown in figure 22. The still and streak camera records are given in figure 23. A summary of the analysis of this shot is presented in Table XVI. The average delay of three control assemblies, consisting of PVA/PETN composites but no Comp B, was  $1.77 \mu\text{sec}$  ( $1.74 - 1.78$ ). The over-all jitter in delay for all five tests with this type of composite assembly is  $0.05 \mu\text{sec}$ . Thus it is apparent that the jitter of some  $0.20$  to  $0.25 \mu\text{sec}$  for the plane wave system is considerably larger than the jitter in the lead azide/PETN composites. The jitter for Pyrex covered lead azide assemblies (45 results) are more nearly comparable to the jitters observed in shot 9022. It is significant that the observed delays, corrected for Comp B transit time, are shortest directly under an azide/PETN assembly and increase linearly with radial distance to the center of the nearest composite assembly. It is possible that a better linear fit results if the radial distance is measured from the nearest portion, rather than the center, of the nearest composite. The scatter in results does not permit a clear distinction between these two approaches. It is interesting that even directly under a composite assembly the average delay is  $1.97 \mu\text{sec}$  rather than the  $1.77 \mu\text{sec}$  measured for controls. Transit times through the Comp B are based on an average Comp B detonation velocity of  $7.8 \text{ mm}/\mu\text{sec}$ . To account for the above difference of  $0.20 \mu\text{sec}$  an unrealistically low Comp B detonation velocity of  $6.9 \text{ mm}/\mu\text{sec}$  would have to be assumed. It seems more likely that the  $0.20 \mu\text{sec}$  represents a delay in the initiation of Comp B. An extrapolation of the results of Campbell *et al.*<sup>21</sup> supports this point of view. The delay in Comp B initiation might explain some of the larger than expected jitters. Probably better control of the intimacy of contact between composite and Comp B is required.





Figure 23 STILL AND STREAK CAMERA  
RECORD OF PLANE WAVE  
DEMONSTRATION SHOT

Table XVI  
PLANE WAVE DEMONSTRATION; SUMMARY OF  
ANALYSIS OF SHOT 9022\*

LOCATION	READINGS	AVG DELAY <sup>†</sup> ( $\mu$ sec)	MAX SPREAD ( $\mu$ sec)
Over pellets 1.96 x 1.96 inches <sup>§</sup>	48	1.97	1.86-2.10
Between pellets (horizontal) <sup>Δ</sup> 2.09 x 2.09 inches <sup>§</sup>	47	2.03	1.93-2.15
Between pellets (vertical) <sup>Δ</sup> 2.19 x 1.96 inches <sup>§</sup>	53	2.02	1.92-2.14
Between pellets (vertical and horizontal) <sup>Δ</sup> 2.19 x 2.09 inches <sup>§</sup>	46	2.07	1.96-2.16
Across pellet face 0.312 inch diam	14	0.048	0.033-0.087

\* See figures 22 and 23 for schematic diagrams of shot.

<sup>†</sup> These are for azide/PETN composite assemblies of azide height of 44 mils (42-47), azide density 3.03 g/cc (2.86-3.16), PETN height 158 mils (154-162), PETN density 1.34 g/cc (1.29-1.43). All corrected for a Comp B transit time of 1.64  $\mu$ sec.

<sup>§</sup> Comp B area.

<sup>Δ</sup> 0.25 inch from center of nearest pellet.

<sup>Δ</sup> 0.35 inch from center of nearest pellet.

The results of shot 8792 are in agreement with those just discussed. In this shot, one array of composites was in 0.500-inch-O.D. sleeves rather than 0.308-inch-O.D. sleeves. For this array, as expected, the Comp B between composite assemblies lagged behind that directly under the composite even more than indicated above.

#### b. POSSIBLE USES OF THE FLASH-BOMB SYSTEM FOR PLANE WAVE GENERATORS

A conventional plane wave generator is required to produce a plane shock in argon for the suggested lead azide-argon flash-bomb surface initiation system. At first glance, therefore, the suggested surface-initiation system would appear to present no advantages for plane-surface initiation. However many conventional plane wave generators do not have a uniform pressure distribution across their surface. In some applications (driving plates, for example) a uniform pressure distribution would be very advantageous. The suggested system would have a uniform pressure distribution.

Conventional plane wave generators for surfaces of any appreciable size usually contain several pounds of explosive. This may be a serious drawback in certain applications (low impulsive loading of test structure). The suggested system can overcome this by:

- (1) having an argon container in the form of a frustum of a pyramid with relatively small conventional plane wave generator initiating a much larger, but less massive, azide surface, and
- (2) using a mirror and barricade arrangement to deliver radiant energy from a big conventional plane wave generator to a thin lead-azide surface in contact with the test structure, without damage to the test structure from the shock energy of the conventional plane wave generator.

Since  $B\tau$  is constant (Table XIV) and the jitter is generally a fixed percentage of  $\tau$  [Sec. 3,a(1)] it is desirable to keep  $\tau$  small. This means that neither system (1) or (2) can be used for illuminating very large surface areas by a small source. Shot 9253 [Table VI and Sec. 3,a(2)] indicates that at least a four-fold increase in area is realizable by system (1) if the front surface confinement is well controlled. System (2) has not been demonstrated experimentally but it is believed to be entirely feasible.

#### c. INITIATION OF CURVED SURFACES

A demonstration of the applicability of the suggested system to the initiation of curved surfaces has not been made because of the unavailability of uniform azide sheets (discussed below). Some results of interest with tilted lead azide assemblies are shown in Table XVII. For Pyrex windows and tilt angles of up to  $30^\circ$  from the vertical there appears to be no dependence of initiation delay on tilt angle. This is very encouraging since it indicates that the suggested system is applicable to slightly curved surfaces. To compensate for greater curvature it may be necessary to place appropriate filters over portions of the curved surface to keep  $B\tau$  nearly constant. It is not apparent why the initiation delays for tilt angles greater than  $30^\circ$  for Pyrex windows, and even at about  $19^\circ$  for crown-glass windows, appear to depend on the projected area of the azide surface (cosecant of tilt angle). More information is needed.

Table XVII  
INITIATION DELAY FOR PVA LEAD AZIDE ASSEMBLIES  
TILTED TOWARD THE COMP B

SHOT NO.	OBSERVATIONS	CONFINEMENT	ANGLE OF TILT = $\theta$ (degrees)	AVG. DELAY = $\tau$ ( $\mu\text{sec}$ )	RANGE	$\tau \cos \theta$
7859	2	Crown <sup>a</sup>	0	1.55	1.52-1.59	--
7859	2	Crown <sup>a</sup>	32	1.76	1.74-1.78	1.49
8580	7	Pyrex	0	1.03	0.97-1.10	--
8580	2	Pyrex	22	1.00	1.00-1.00	--
8580	2	Pyrex	30	1.27	1.26-1.27	1.10
9043	2	Crown	0	0.99	0.95-1.02	--
9043	2	Crown	18.7	1.09	1.05-1.14	1.03
9043	3	Pyrex <sup>b</sup>	0	0.91	0.88-0.94	--
9043	2	Pyrex <sup>b</sup>	21.5	0.95	0.94-0.96	--
9043	2	Pyrex <sup>b</sup>	26.5	0.91	0.88-0.94	--

<sup>a</sup> Measured from vertical.

<sup>b</sup> From Ref. 1

<sup>c</sup> PVA/PETN composite assemblies.

#### d. LEAD AZIDE SHEET

Section 4,a makes it obvious that the success of the suggested system of surface initiation will depend on the availability of a continuous and uniform layer of lead azide. It is very encouraging (Table X) that considerable amounts of impurity (binder for the sheet azide) do not affect initiation delay. Some results are given in Table XVIII for very porous and rather nonuniform home-made azide sheet in which some segregation of azide and binder exists. These results leave no doubt that sheet azide can be flash-bomb initiated, but they do point out the necessity of having the sheet azide much more uniform than that made according to the procedure outlined in Sec. 2,b(1). Quite likely the procedure for providing front-surface confinement for sheet azide needs improvement. The Du Pont Company has made sheet azide. Since their preparation involved rolling of the sheet, it is to be expected that their material is much more uniform than the sheet made in this laboratory. Unfortunately, the Du Pont Company has experienced an accident in the handling of their sheet azide.\*

\* Consequently, the release of this sheet azide has been suspended until the causes of the accident are established.

Table XVIII  
INITIATION DELAYS FOR 90/10 PVA LEAD AZIDE/FORMVAR SHEET\*

SHOT	SHEET THICKNESS (mils)	SURFACE FACING FLASH† BOMB	INITIATION DELAY§ (μsec)	
			Sheet	Control
9252	46	Azide	0.88(1.16)	0.73
9252	46	Azide	1.26(1.16)	0.73
9042	31	Probably azide	1.04(0.78)	0.87
9042	25	Probably azide	1.15(0.63)	0.87
9042	28	Probably azide	1.23(0.71)	0.87

\* Sheet density about 1.3 g/c.c.

† Microscopic examination revealed segregation of azide and formvar.

§ Sheets had Pyrex windows; they were placed on PETN assemblies of 1.32 g/c.c., correction for transit time of PETN was taken as 0.37 μsec; the bracketed terms are the estimated azide transit times; controls were standard, Pyrex window, PVA lead azide assemblies.

It is felt that the success of the development of a practical system of surface initiation hinges on obtaining uniform azide sheet from Du Pont, or else setting up a fairly elaborate procedure for making such sheets.

#### e. IMPROVED FRONT-SURFACE CONFINEMENT

In Sec. 3,a(2), the dependence of delay jitter on intimacy of contact between front-surface confinement (window) and azide was demonstrated. In view of this dependence, and also because of ease of application in a practical system, it is very desirable to develop a transparent paint which can be sprayed or brushed over an azide surface. Preliminary trials with a nitrocellulose lacquer were unsuccessful.<sup>1</sup> Formvar (the binder in the home-made sheet azide) can be deposited as a tough clear layer. Unfortunately, the clear Formvar window was found to absorb radiation in the region where most of the lead azide absorption occurs.

#### f. EXPLOSIVE TRAIN

In many possible applications of a practical surface initiation system, a more powerful and less sensitive main charge than lead azide may be desirable. As shown in Sec. 4,a, lead azide—PETN composites will reliably initiate Comp B, which appears to be the logical choice for main charge since it is castable, machinable, and relatively safe. A practical explosive train might consist of lead azide sheet, 95/5



PETN/binder sheet (available from Du Pont and claimed by them to be initiated by their lead azide sheet), Du Pont EL-506D sheet explosive (not initiated directly by lead azide), and Comp B. The last two constituents of the train are relatively safe to handle and could be assembled together and then mated to the azide sheet and sensitive PETN sheet (remotely if necessary) just prior to the shot.

#### g. FLASH-BOMBS

To initiate large, highly curved surfaces it may be necessary to use more than one flash-bomb. In this case, the energy flux and simultaneity of the flash-bombs would have to be controlled carefully. Considerable shot-to-shot variation in peak light intensity (see Table VI) has been encountered. Possibly this variation was caused by pockets of air not completely flushed out by the flowing argon. To eliminate this possible cause, it may be desirable to evacuate the containers prior to flushing them with argon.

Rise times to peak intensity appear to be quite reproducible (Table IV). It would be desirable, however, to shorten the rise since this would increase  $B$  and shorten  $\tau$ . This can be accomplished, at considerable expense, by replacing the argon with krypton or xenon (Table IV) which would also raise the peak intensity. A higher detonation velocity pad (HMX for example) in the plane wave generator would also be beneficial (if such a pad drives the shock through argon at a higher velocity) because time to reach peak argon emissivity would be reduced, (Eq. 5). For the same reason it is expected that argon under pressure (several atmospheres) would shorten rise times. Mechanical shuttering (placing a thin opaque membrane, which is destroyed by the shock, between the Comp B pad and the azide) does not appear to decrease rise times. In several small-scale shots, mechanical shuttering, if anything, slightly increased rise times.

#### h. RECOMMENDATIONS FOR FURTHER STUDY

Before a practical system of surface initiation is achieved it is imperative to obtain uniform lead-azide sheet. It is also necessary to develop some system, probably in the form of a transparent paint, of confining the surface of the azide sheet facing the flash-bomb. Provided lead azide sheet is available, the rest of the explosive train

should present no problems. For certain proposed systems reproducibility (peak intensity and rise times) of the flash-bombs will have to be improved. Some further study of the effect of tilt of the azide surface (with respect to the plane shock in the flash-bomb) on the initiation delay will also be required, before highly curved geometries can be surface initiated. It might be desirable to investigate the possibility of replacing lead azide with a sensitive liquid explosive, for example, nitroglycerine. For a liquid explosive close front-surface confinement is readily achieved. The explosive can be made to assume any desired contour. Liquids such as nitroglycerine can be made highly light-absorbent by dissolving in them minute quantities of organic black dyes. It is not known, however, whether rapid self-heating, even in an explosive as sensitive as nitroglycerine, can lead to detonation in times short enough to allow the delay jitter to be sufficiently small.

## REFERENCES

1. Roth, J., "Research Study on the Surface Initiation of Explosives," Final Report, AFSWC-TR-61-59, 1961.
2. Bond, J. W., "The Structure of a Shock Front in Argon," Los Alamos Scientific Lab., LA 1893, 1954.
3. Brink, D. E., Hurst, R., "Plane Wave Generators," SRI Poulter Lab. Tech. Report, 001-58, 1958.
4. Cook, M. A., *The Science of High Explosives*, ACS Monograph, p. 45, 1958.
5. Pivonsky, M. A., and Nagel, M. R., *Tables of Blackbody Radiation Functions*, Macmillan Co., N.Y., 1961.
6. Zeldovich, Ia., B., *J. Exptl. Theoret. Phys. (U.S.S.R.)* 32, 1028, 1957.
7. Model I., Sh., *Soviet Phys. JETP*, Vol. 5, No. 4, 589, 1957.
8. Private Communication from the Ensign-Bickford Co.
9. Hardy, A. C., and Perrin, F. H., *The Principles of Optics*, pp. 410-411, McGraw Hill, N.Y., 1932.
10. The Transmission Curve for 395°C was taken from *N.B.S. Handbook*, Vol. III, pp. 421-428, 1961.
11. Cook, M. A., op. cit., p. 180.
12. Garner, W. E., and Gomm, A. S., *J. Chem. Soc.*, 2123, 1931.
13. Ubbelohde, A. R., and Woodward, P., *Phil. Trans. Roy. Soc.*, A241, 228, 1948.
14. Hawkes, A. S., and Winkler, C. A., *Can. J. Research*, 25B, 548, 1947.
15. *Handbook of Chemistry and Physics*, 29th Edition.
16. Evans, B. L., Yoffee, A. D., and Gray, P., *Chem. Rev.*, 59, 559, 1958.
17. Noyes, W. A., and Leighton, P. A., *The Photochemistry of Gases*, p. 151, Reinold, N.Y., 1941.
18. Dodd, J., Final Report, DA-44-009, Eng. 4194.
19. Shreffler, R. G., and Christian, R. H., *J. Appl. Phys.*, 25, No. 3, 324, 1954.
20. Christian, R. H., and Yarger, F. L., *J. Chem. Phys.*, 23, No. 11, 2044, 1955.
21. Campbell, A. W. et al., *Phys. Fluids*, 4, No. 4, 511, 1961.
22. Bagley, C. H., *Rev. Sci. Inst.*, 30, No. 2, 103, 1959.

## APPENDIX

### 1. PRECURSOR IN ARGON SHOCKS

Figure 8 clearly shows a faint luminosity running ahead of the bright, Comp B-generated, shock in argon. Undoubtedly, this phenomenon is the same as that observed by Shreffler and Christian.<sup>19</sup> They attribute the precursor to a high-velocity disturbance propagating along the container walls. They claim that this disturbance is caused by radiation from the highly luminous main shock. The steady precursor propagation velocity of 10 to 10.7 mm/ $\mu$ sec observed in this laboratory is very close to the 11.1 mm/ $\mu$ sec given by Shreffler and Christian.

### 2. THEORETICAL CALCULATION OF THE TEMPERATURE OF SHOCKED ARGON

Bond<sup>2</sup> has derived equations for the temperature  $T_e$  and the compression ratio  $\eta$ , in terms of the shock velocity  $U$  and equilibrium constants for the process,  $A = A^+ + e^-$ . His calculations are for an initial pressure of 59.4 cm Hg (ambient pressure at Los Alamos). He shows how the equilibrium constants vary with initial pressure. The tabulation below gives Bond's original results, our results using Bond's equations and data to correct to an ambient pressure of 76 cm Hg, and a calculation according to Bond's methods but varying,  $x$ , the equilibrium fraction of argon ionized to bring  $T_e$  to the observed value of 29000°K.

	$U$ (mm/ $\mu$ sec)	$P_0$ (cm Hg)	$x$	$\eta$	$T_e$ (°K)
Bond	8.3	59.4	0.34	9.5	23,500
This report	8.3	76	0.33	9.3	23,900
This report	8.3	76	0.265	7.9	29,000
Experimental <sup>20</sup>	8.26	59.4	--	9.4 $\pm$ 0.5	--

This tabulation indicates that a relatively small change in  $x$  will bring  $(T_e)_{obs}$  and  $(T_e)_{calc}$  into agreement. However this small change in  $x$  appears to worsen the agreement between  $(\eta)_{obs}$  and  $(\eta)_{calc}$ .

Incidentally, Bond's calculations indicate that both translational and ionization equilibria for shocked argon are attained in several nanoseconds.

The value of  $T_e$  of 26,500 K given in Ref. 1 is based on calculations for an argon "shock velocity" of 9.6 mm/ $\mu$ sec. It is now apparent that this shock velocity was an average precursor propagation velocity (Appendix A).

DISTRIBUTION

No. cys

HEADQUARTERS USAF

1	Hq USAF (AFRDP), Wash 25, DC
1	Hq USAF (AFORQ), Wash 25, DC
1	Hq USAF (AFTAC), Wash 25, DC
	AFOAR, Bldg T-D, Wash 25, DC
1	(RRONN)
1	(RROSA, Col Boreske)
1	(RROSP, Lt Col Atkinson)
1	AFOSR, Bldg T-D, Wash 25, DC
1	ARL (RRLO) ATTN: Mr. Cady, ARO, Wright-Patterson AFB, Ohio

MAJOR AIR COMMANDS

	AFSC, Andrews AFB, Wash 25, DC
1	(SCT)
1	(SCT-2)
1	(SCLAS, Col P. F. English)
	SAC, Offutt AFB, Nebr
1	(OA) ATTN: Dr. E. A. Jackson
1	(OAWS)
1	AUL, Maxwell AFB, Ala
1	USAFIT (USAF Institute of Technology), Wright-Patterson AFB, Ohio

AFSC ORGANIZATIONS

	ASD, Wright-Patterson AFB, Ohio
2	(ASAPRL)
1	(ASRMDS-1, Mr. Janik)
1	RTD (RTN-W, Maj Munyon), Bolling AFB, Wash 25, DC
	BSD, Norton AFB, Calif
1	(BSR)
1	(BSRD, Lt Col Caseria)
1	(BSRVE, Lt Col Parker)
1	(BSLA)

## DISTRIBUTION (cont'd)

No. cys

1	(BSTD)
1	(BSAT)
1	SSD, AF Unit Post Office, Los Angeles 45, Calif
	ESD, Hanscom Fld, Bedford, Mass
2	(ESAT)
1	(ESDL)
1	(ESDS)
1	AF Msl Dev Cen (RRRT), Holloman AFB, NM
1	AFFTC (FTFT), Edwards AFB, Calif
1	AFMTC (MU-135), Patrick AFB, Fla
1	APGC (PGAPI), Eglin AFB, Fla
1	RADC (Document Library), Griffiss AFB, NY

## KIRTLAND AFB ORGANIZATIONS

1	AFSWC (SWEH), Kirtland AFB, NM
	AFWL, Kirtland AFB, NM
20	(WLL)
2	(WLRPA)
1	(WLRPL)
1	(WLRPT)
1	(WLA)
1	ADC (ADSWO), Special Weapons Office, Kirtland AFB, NM
1	ATC Res Rep (SWN), AFSWC, Kirtland AFB, NM
1	AFLC, Albuquerque Ln Ofc (MCSWQ), AFSWC, Kirtland AFB, NM
1	SAC Res Rep (SWL), AFSWC, Kirtland AFB, NM
1	TAC Liaison Office (TACLO-S), AFSWC, Kirtland AFB, NM
1	US Naval Weapons Evaluation Facility (NWEF) (Code 404), Kirtland AFB, NM

## OTHER AIR FORCE AGENCIES

Director, USAF Project RAND, via: Air Force Liaison Office,  
The RAND Corporation, 1700 Main Street, Santa Monica, Calif

1	(RAND Library)
1	(Dr. Olen Nance, Physics Department)

DISTRIBUTION (cont'd)

No. cys

- 1 (Maj J. A. Welch, USAF)
- 1 (Mr. Jack Whitener)
- 1 Aerospace Defense Systems Office (ADO), ATTN: ADSO, AF Unit  
Post Office, Los Angeles, Calif

ARMY ACTIVITIES

- 1 Chief of Research and Development, Department of the Army,  
ATTN: Maj Baker, Wash 25, DC
- 1 US Army Materiel Command, Harry Diamond Laboratories,  
(ORDTL 06.33, Technical Library), Wash 25, DC
- 1 Commanding Officer, US Army Combat Developments Command,  
Nuclear Group, Ft Bliss 16, Tex.
- 1 ARGMA Liaison Office, Bell Telephone Labs, Whippany, NJ
- 1 Redstone Scientific Information Center, US Army Missile Command  
(Tech Library), Redstone Arsenal, Ala
- Director, Ballistic Research Laboratories, Aberdeen Proving  
Ground, Md
- 1 (Mr. Ed Bailey)
- 1 (Dr. Coy Glass)
- Commanding Officer, Picatinny Arsenal, Samuel Feltman  
Ammunition Laboratories, Dover, NJ
- 1 (ORDBB-TV8)
- 1 (Mr. Murray Weinstein)
- 1 Operations Research Office, John Hopkins University (Document  
Control Office), 6935 Arlington Rd., Bethesda, Md., Wash 14, DC
- 1 US Army Research Office, ATTN: Richard O. Ulsh, Box CM,  
Durham, NC
- 1 Director, Army Research Office, Arlington Hall Sta, Arlington, Va
- 1 Director, US Army Engineer Research & Development Laboratories,  
ATTN: Tech Documents Center, Ft Belvoir, Va

NAVY ACTIVITIES

- 1 Chief of Naval Operations, Department of the Navy, ATTN: OP-36,  
Wash 25, DC
- 1 Chief of Naval Research, Department of the Navy, ATTN: Mr.  
James Winchester, Wash 25, DC



DISTRIBUTION (cont'd)

No. cys

- 1 Chief, Bureau of Naval Weapons, Department of the Navy, Wash 25, DC
- 1 Commanding Officer, Naval Research Laboratory, Wash 25, DC
- 1 Commander, Naval Ordnance Laboratory, ATTN: Dr. Leonard Rudlin, White Oak, Silver Spring, Md
- 2 Director, Special Projects, Department of the Navy, ATTN: Mr. D. R. Williams, Wash 25, DC

OTHER DOD ACTIVITIES

- Chief, Defense Atomic Support Agency, Wash 25, DC
- 2 (Document Library)
- 1 (DASARA, Lt Col Singer)
- 1 Commander, Field Command, Defense Atomic Support Agency (FCAG3, Special Weapons Publication Distribution), Sandia Base, NM
- 5 Director, Weapon Systems Evaluation Group, Room 2E1006, The Pentagon, Wash 25, DC
- 1 (Lt Col Roy Weidler)
- 1 Director, Defense Research & Engineering, The Pentagon, Wash 25, DC
- 1 DASA Data Center, Tempo-General Electric Co., P.O. Drawer QQ, Santa Barbara, Calif
- 20 Hq Defense Documentation Center for Scientific and Technical Information (DDC), Arlington Hall Sta, Arlington 12, Va

AEC Activities

- 1 US Atomic Energy Commission Headquarters Library, Reports Section, Mail Station G-017, Wash 25, DC
- 2 Sandia Corporation (Technical Library), Sandia Base, NM
- 2 Sandia Corporation (Technical Library), P. O. Box 969, Livermore, Calif
- 1 Chief, Division of Technical Information Extension, US Atomic Energy Commission, Box 62, Oak Ridge, Tenn
- 1 University of California Lawrence Radiation Laboratory (Technical Information Division), P. O. Box 808, Livermore, Calif
- 1 University of California Lawrence Radiation Laboratory, (Technical Information Division) ATTN: Dr. R. K. Wakerling, Berkely 4, Calif

DISTRIBUTION (cont'd)

No. cys

4 Director, Los Alamos Scientific Laboratory (Helen Redman,  
Report Library), P. O. Box 1663, Los Alamos, NM  
1 Brookhaven National Laboratory, Upton, Long Island, NY  
1 Argonne National Laboratory (Tech Library), Argonne, Ill  
1 Oak Ridge National Laboratory (Tech Library), Oak Ridge, Tenn

OTHER

1 Institute for Defense Analysis, Room 2B257, The Pentagon,  
Wash 25, DC  
1 Institute of the Aerospace Sciences, Inc., 2 East 64th Street,  
New York 21, NY  
Aeronutronic, Division of Ford Motor Co., Newport Beach, Calif  
1 (Dr. Montgomery Johnson)  
1 (Dr. R. G. Allen)  
1 (Dr. R. Grandey)  
1 E. H. Plesset Assoc., Inc., ATTN: Dr. Harris Mayer, 1281  
Westwood Blvd., Los Angeles 24, Calif  
Stanford Research Institute, Menlo Park, Calif  
1 (Dr. Duvall)  
1 (Dr. Fowles)  
1 (Dr. Abrahamson)  
1 General Electric Aero Sciences Lab, ATTN: Dr. Steg, 3198  
Chestnut Street, Philadelphia, Pa  
AVCO Corp, Research & Advanced Dev. Div., 201 Lowell Street,  
Wilmington, Mass  
1 (Dr. W. L. Bade)  
2 (Dr. Dean Morgan)  
1 Aerojet-General Corp., ATTN: Mr. M. Wagner, 1711 S. Woodruff  
Avenue, Downey, Calif  
1 The Boeing Company, Aerospace Division, ATTN: Dr. Penning,  
Seattle 14, Wash  
1 Lockheed Missile & Space Company, ATTN: Mr. Milton McGuire,  
Sunnyvale, Calif  
1 Southwest Research Institute, ATTN: Dr. G. Nevill, 8500 Culebra  
Road, San Antonio 6, Tex

DISTRIBUTION (cont'd)

No. cys

- 1 Technical Operations, Inc., ATTN: Dr. Kofsky, Burlington, Mass
- 1 Kaman Aircraft Corp., Nuclear Division, ATTN: Dr. A. P. Bridges, Colorado Springs, Colo
- 1 Space Technology Labs, ATTN: Dr. Herman Leon & Mr. Jackson Maxey, P. O. Box 95001, Los Angeles 45, Calif
- Aerospace Corp, Los Angeles 45, Calif
- 1 (Dr. Domenic Bitondo)
- 1 (Dr. George Welch)
- 1 (Dr. Robert Cooper)
- 1 (Mr. H. C. Sullivan)
- 1 (Dr. W. Loh)
- 1 (Dr. G. A. E. Graham)
- 1 General Electric, Defense Systems, ATTN: Mr. A. Sinisgalli, Atlantic Building, Syracuse, NY
- 1 General Electric Company, MSD, ATTN: Mr. J. Spencer, 3198 Chestnut Street, Philadelphia 4, Pa
- 1 Battelle Memorial Institute, ATTN: Battelle DEFENDER, 505 King Avenue, Columbus 1, Ohio
- 1 Massachusetts Institute of Technology, Aeroelastic & Structures Research Laboratory, ATTN: Mr. Walter Herrman, Cambridge, Mass
- 1 Official Record Copy (WLRPA, Lt Haycock)

<p>Air Force Special Weapons Center, Kirtland AF Base, New Mexico Rpt. No. AFSC-TR-63-49. RESEARCH STUDY ON THE SURFACE INITIATION OF EXPLOSIVES. Final Report, June 1963. 32 p. incl illus, tables, 22 refs.</p> <p>Unclassified Report</p> <p>To fill a continued military demand for controlled explosive wave shaping this study has been undertaken to establish basic conditions for explosive systems capable of being initiated uniformly over their entire surface, and to demonstrate the functioning of the proposed system for simple geometries. This investigation is a continuation of that started under AFSC TR-61-59. The proposed system consists of PVA lead azide initiated by radiation from an argon flash bomb. In addition to lead azide, the suggested</p>	<ol style="list-style-type: none"> <li>1. Explosives</li> <li>2. Initiators</li> <li>3. Lead azide</li> <li>4. Light sources</li> <li>5. Radiation</li> <li>I. AFSC Project 5776, Task 577601</li> <li>II. Contract AF 29(601)-5134</li> <li>III. Stanford Research Inst., Poulter Labs., Menlo Park, Calif.</li> <li>IV. Secondary Rpt No. SRI Project PGU-3997</li> <li>V. In DDC collection</li> </ol>	<p>Air Force Special Weapons Center, Kirtland AF Base, New Mexico Rpt. No. AFSC-TR-63-49. RESEARCH STUDY ON THE SURFACE INITIATION OF EXPLOSIVES. Final Report, June 1963. 32 p. incl illus, tables, 22 refs.</p> <p>Unclassified Report</p> <p>To fill a continued military demand for controlled explosive wave shaping this study has been undertaken to establish basic conditions for explosive systems capable of being initiated uniformly over their entire surface, and to demonstrate the functioning of the proposed system for simple geometries. This investigation is a continuation of that started under AFSC TR-61-59. The proposed system consists of PVA lead azide initiated by radiation from an argon flash bomb. In addition to lead azide, the suggested</p>	<ol style="list-style-type: none"> <li>1. Explosives</li> <li>2. Initiators</li> <li>3. Lead azide</li> <li>4. Light sources</li> <li>5. Radiation</li> <li>I. AFSC Project 5776, Task 577601</li> <li>II. Contract AF 29(601)-5134</li> <li>III. Stanford Research Inst., Poulter Labs., Menlo Park, Calif.</li> <li>IV. Secondary Rpt No. SRI Project PGU-3997</li> <li>V. In DDC collection</li> </ol>
<p>Air Force Special Weapons Center, Kirtland AF Base, New Mexico Rpt. No. AFSC-TR-63-49. RESEARCH STUDY ON THE SURFACE INITIATION OF EXPLOSIVES. Final Report, June 1963. 32 p. incl illus, tables, 22 refs.</p> <p>Unclassified Report</p> <p>To fill a continued military demand for controlled explosive wave shaping this study has been undertaken to establish basic conditions for explosive systems capable of being initiated uniformly over their entire surface, and to demonstrate the functioning of the proposed system for simple geometries. This investigation is a continuation of that started under AFSC TR-61-59. The proposed system consists of PVA lead azide initiated by radiation from an argon flash bomb. In addition to lead azide, the suggested</p>	<ol style="list-style-type: none"> <li>1. Explosives</li> <li>2. Initiators</li> <li>3. Lead azide</li> <li>4. Light sources</li> <li>5. Radiation</li> <li>I. AFSC Project 5776, Task 577601</li> <li>II. Contract AF 29(601)-5134</li> <li>III. Stanford Research Inst., Poulter Labs., Menlo Park, Calif.</li> <li>IV. Secondary Rpt No. SRI Project PGU-3997</li> <li>V. In DDC collection</li> </ol>	<p>Air Force Special Weapons Center, Kirtland AF Base, New Mexico Rpt. No. AFSC-TR-63-49. RESEARCH STUDY ON THE SURFACE INITIATION OF EXPLOSIVES. Final Report, June 1963. 32 p. incl illus, tables, 22 refs.</p> <p>Unclassified Report</p> <p>To fill a continued military demand for controlled explosive wave shaping this study has been undertaken to establish basic conditions for explosive systems capable of being initiated uniformly over their entire surface, and to demonstrate the functioning of the proposed system for simple geometries. This investigation is a continuation of that started under AFSC TR-61-59. The proposed system consists of PVA lead azide initiated by radiation from an argon flash bomb. In addition to lead azide, the suggested</p>	<ol style="list-style-type: none"> <li>1. Explosives</li> <li>2. Initiators</li> <li>3. Lead azide</li> <li>4. Light sources</li> <li>5. Radiation</li> <li>I. AFSC Project 5776, Task 577601</li> <li>II. Contract AF 29(601)-5134</li> <li>III. Stanford Research Inst., Poulter Labs., Menlo Park, Calif.</li> <li>IV. Secondary Rpt No. SRI Project PGU-3997</li> <li>V. In DDC collection</li> </ol>

<p>explosive train consists of PETN and Comp B. Uniformity of initiation in this train is quite good, but can undoubtedly be improved if lead aside in sheet form becomes available. Because sheet aside was unavailable, the applicability of the proposed system has not been demonstrated for curved explosive surfaces, but it is believed that surface initiation of curved surfaces can be achieved.</p>		<p>explosive train consists of PETN and Comp B. Uniformity of initiation in this train is quite good, but can undoubtedly be improved if lead aside in sheet form becomes available. Because sheet aside was unavailable, the applicability of the proposed system has not been demonstrated for curved explosive surfaces, but it is believed that surface initiation of curved surfaces can be achieved.</p>	
<p>explosive train consists of PETN and Comp B. Uniformity of initiation in this train is quite good, but can undoubtedly be improved if lead aside in sheet form becomes available. Because sheet aside was unavailable, the applicability of the proposed system has not been demonstrated for curved explosive surfaces, but it is believed that surface initiation of curved surfaces can be achieved.</p>	○	<p>explosive train consists of PETN and Comp B. Uniformity of initiation in this train is quite good, but can undoubtedly be improved if lead aside in sheet form becomes available. Because sheet aside was unavailable, the applicability of the proposed system has not been demonstrated for curved explosive surfaces, but it is believed that surface initiation of curved surfaces can be achieved.</p>	○

<p>Air Force Special Weapons Center, Kirtland AF Base, New Mexico Rpt. No. AFSCC-DR-63-49. RESEARCH STUDY ON THE SURFACE INITIATION OF EXPLOSIVES. Final Report, June 1963. 32 p. incl illus, tables, 22 refs.</p> <p>Unclassified Report</p> <p>To fill a continued military demand for controlled explosive wave shaping this study has been undertaken to establish basic conditions for explosive systems capable of being initiated uniformly over their entire surface, and to demonstrate the functioning of the proposed system for simple geometries. This investigation is a continuation of that started under AFSCC TR-61-39. The proposed system consists of PVA lead aside initiated by radiation from an argon flash bomb. In addition to lead aside, the suggested</p>	<p>Explosives Initiators Lead aside Light sources Radiation Surface explosions AFSCC Project 5776, Task 577601 Contract AF 29(601)-5134 Stanford Research Inst., Poulter Labs., Menlo Park, Calif. Secondary Rpt No. SRI Project PCU-3977 In DDC collection</p>	<p>1. Explosives 2. Initiators 3. Lead aside 4. Light sources 5. Radiation 6. Surface explosions I. AFSCC Project 5776, Task 577601 II. Contract AF 29(601)-5134 III. Stanford Research Inst., Poulter Labs., Menlo Park, Calif. IV. Secondary Rpt No. SRI Project PCU-3977 V. In DDC collection</p>
<p>Air Force Special Weapons Center, Kirtland AF Base, New Mexico Rpt. No. AFSCC-DR-63-49. RESEARCH STUDY ON THE SURFACE INITIATION OF EXPLOSIVES. Final Report, June 1963. 32 p. incl illus, tables, 22 refs.</p> <p>Unclassified Report</p> <p>To fill a continued military demand for controlled explosive wave shaping this study has been undertaken to establish basic conditions for explosive systems capable of being initiated uniformly over their entire surface, and to demonstrate the functioning of the proposed system for simple geometries. This investigation is a continuation of that started under AFSCC TR-61-39. The proposed system consists of PVA lead aside initiated by radiation from an argon flash bomb. In addition to lead aside, the suggested</p>	<p>Explosives Initiators Lead aside Light sources Radiation Surface explosions AFSCC Project 5776, Task 577601 Contract AF 29(601)-5134 Stanford Research Inst., Poulter Labs., Menlo Park, Calif. Secondary Rpt No. SRI Project PCU-3977 In DDC collection</p>	<p>1. Explosives 2. Initiators 3. Lead aside 4. Light sources 5. Radiation 6. Surface explosions I. AFSCC Project 5776, Task 577601 II. Contract AF 29(601)-5134 III. Stanford Research Inst., Poulter Labs., Menlo Park, Calif. IV. Secondary Rpt No. SRI Project PCU-3977 V. In DDC collection</p>

<p>explosive train consists of FPM and Comp 3. Uniformity of initiation in this train is quite good, but can undoubtedly be improved if lead azide in sheet form becomes available. Because sheet azide was unavailable, the applicability of the proposed system has not been demonstrated for curved explosive surfaces, but it is believed that surface initiation of curved surfaces can be achieved.</p>		<p>explosive train consists of FPM and Comp 3. Uniformity of initiation in this train is quite good, but can undoubtedly be improved if lead azide in sheet form becomes available. Because sheet azide was unavailable, the applicability of the proposed system has not been demonstrated for curved explosive surfaces, but it is believed that surface initiation of curved surfaces can be achieved.</p>	
<p>explosive train consists of FPM and Comp 3. Uniformity of initiation in this train is quite good, but can undoubtedly be improved if lead azide in sheet form becomes available. Because sheet azide was unavailable, the applicability of the proposed system has not been demonstrated for curved explosive surfaces, but it is believed that surface initiation of curved surfaces can be achieved.</p>		<p>explosive train consists of FPM and Comp 3. Uniformity of initiation in this train is quite good, but can undoubtedly be improved if lead azide in sheet form becomes available. Because sheet azide was unavailable, the applicability of the proposed system has not been demonstrated for curved explosive surfaces, but it is believed that surface initiation of curved surfaces can be achieved.</p>	